UNCLASSIFIED

AD NUMBER

AD-479 786

NEW LIMITATION CHANGE

TO

DISTRIBUTION STATEMENT - A

Approved for public release;
distribution is unlimited.

LIMITATION CODE: 1

FROM

DISTRIBUTION STATEMENT - B

LIMITATION CODE: 3

AUTHORITY

AF FLT Dynamics Lab; 24 Jan 1973

19990604249

THIS PAGE IS UNCLASSIFIED

THE EFFECTIVE POROSITY OF PARACHUTE CLOTH

H. G. HEINRICH

UNIVERSITY OF MINNESOTA

TECHNICAL REPORT AFFDL-TR-65-102

JANUARY 1966

AIR FORCE FLIGHT DYNAMICS LABORATORY
RESEARCH AND TECHNOLOGY DIVISION
AIR FORCE SYSTEMS COMMAND
WRIGHT-PATTERSON AIR FORCE BASE, OHIO

NOTICES

When Government drawings, specifications, or other data are used for any purpose other than in connection with a definitely related Government procurement operation, the United States Government thereby incurs no responsibility nor any obligation whatsoever; and the fact that the Government may have formulated, furnished, or in any way supplied the said drawings, specifications, or other data, is not to be regarded by implication or otherwise as in any manner licensing the holder or any other person or corporation, or conveying any rights or permission to manufacture, use, or sell any patented invention that may in any way be related thereto.

THE EFFECTIVE POROSITY OF PARACHUTE CLOTH

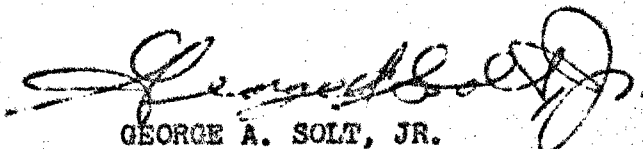*H. G. HEINRICH*

UNIVERSITY OF MINNESOTA

FOREWORD

This report was prepared by the Department of Aeronautics and Engineering Mechanics of the University of Minnesota in compliance with U. S. Air Force Contract No. AF 33(657)-11184, "Theoretical Deployable Aerodynamic Decelerator Investigations," Task 606503, "Parachute Aerodynamics and Structures," Project 6065, "Performance and Design of Deployable Aerodynamic Decelerators."

The work accomplished under this contract was sponsored jointly by U. S. Army Natick Laboratory, Department of the Army; Bureau of Aeronautics and Bureau of Ordnance, Department of the Navy; and Air Force Systems Command, Department of the Air Force and was directed by a Tri-Service Steering Committee concerned with Aerodynamic Retardation. The work was administered under the direction of the Recovery and Crew Station Branch, Air Force Flight Dynamics Laboratory, Research and Technology Division. Mr. Rudi J. Berndt and Mr. James H. DeWeese were the project engineers.

The author wishes to express his appreciation to the many students of Aerospace Engineering of the University of Minnesota who participated in the accomplishment of this objective and to his associates, Messrs. Eugene L. Haak and Ronald J. Niccum.

The manuscript was released by the author in December 1965 for publication as an RTD technical report.

This technical report was reviewed and is approved.

GEORGE A. SOLT, JR.
Chief, Recovery and Crew Station Branch
AF Flight Dynamics Laboratory

ii

ABSTRACT

Stability, drag, and opening characteristics
of solid cloth parachutes change with altitude. Similar
changes can be observed at a given altitude when the
air permeability or porosity of the cloth is being varied.
In this study it is shown that the porosity of a given cloth
changes effectively with the density and the compressibility
of the air. The effective porosity is related to Reynolds
and Mach numbers and it was found that the flow of air
through the cloth is in general turbulent but may approach
under certain circumstances a laminar flow character.

Tables and graphs showing the effective porosity
of four common types of parachute cloth and of one type
of a Perlon screen with 45% geometric porosity, as well
as equations and coefficients which permit under certain
simplifying assumptions the calculation of the effective
porosity are presented.

TABLE OF CONTENTS

ILLUSTRATIONS

ILLUSTRATIONS (CONT.)

LIST OF TABLES

SYMBOLS

A	area
M	Mach number
P, p	pressure
T	temperature
γ	ratio of specific heat at constant pressure to specific heat at constant temperature
μ	coefficient of viscosity
ρ	density

Subscripts

$(\ )_{cr}$	signifies state at which $M = 1$
$(\ )_{thr}$	signifies throat location
$(\ )_0$	signifies sea level condition
$(\ )_1$	signifies conditions upstream of parachute cloth
$(\ )_2$	signifies conditions downstream of parachute cloth
$(\ )_\infty$	signifies free stream conditions

Additional symbols, when used, are defined in the text.

I. INTRODUCTION

Wind tunnel experiments have shown that the drag and the static stability of parachutes are strongly influenced by the cloth porosity of the parachute canopy. Furthermore, it has been observed that the opening shock of solid cloth parachutes increases with altitude while the oscillations of statically unstable parachutes become more violent (Refs 1 and 2).

Attempts have been made to explain the increase of the opening shock as a consequence of the decrease of the apparent mass and the mass of air included in the parachute canopy with the air density (Ref 3). The variation of the stability behavior of a parachute may in part also be attributed to the effect of the apparent and included masses because the motion of a freely descending parachute is a problem of dynamic stability in which the air masses are significant terms (Ref 4).

If the parachute cloth is considered to be a screen through which, during the use of the parachute, a certain amount of air passes, one may assume that the air permeability or porosity of this screen depends on the Reynolds and Mach number of the flow conditions. Therefore, the observed changes in parachute drag and stability may be caused by Reynolds and Mach number effects, characteristic for the flow of air through the porous cloth. Furthermore, experiments have shown (Ref 5) that the apparent mass of parachutes also depends on the porosity of the canopy material. Therefore, the opening shock and the dynamic stability characteristics of a parachute are probably also affected by the variation of the cloth porosity.

Since the opening shock imposes the maximum stress upon all parts of the parachute, a reliable prediction of the parachute safety factor under various operational conditions also depends on the knowledge of the cloth porosity for the given circumstances.

In view of these circumstances, the opening shock, the stability behavior, the rate of descent and the strength of parachutes can be predicted more reliably if the porosity characteristics of the cloth are satisfactorily known, and the air resistance or the porosity of the parachute material as a function of Mach and Reynolds numbers may actually be the most fundamental parameter in the technology of parachutes.

Therefore, the mechanics of the flow through the cloth is investigated in the first part of the following study, whereas tables and graphs covering a wide range of pressure and density are presented in the latter portion. These porosity-pressure-density data may be used for direct application in parachute performance calculations.

1

II. THE EFFECTIVE POROSITY

The porosity, also called air permeability, is conventionally expressed as the volumetric flow rate of air per unit of area under a specified differential pressure (Ref 6). Figure 1 shows a typical diagram of this nominal porosity versus differential pressure for three commonly used parachute materials. This is in many respects an unsatisfactory way of presentation, and already 20 years ago, Prof. George Madelung, Stuttgart, Germany, suggested that more meaningful definitions and presentations should be introduced.

Another way of presenting the porosity characteristics is the derivation of a drag coefficient as a function of the differential pressure or Reynolds number as, for example, shown in Ref 7.

However, for parachute filling time and opening shock calculations, one has to solve a mass balance equation in which one compares the volume of air flowing into the canopy with the air which escapes through the porous canopy material (Ref 8). This process has lead to the establishment of a dimensionless term which is the ratio of the average velocity, U, through the porous surface to a conveniently defined free stream velocity, V. The fictitious velocity, V, is derived from the assumption that the pressure differential across the cloth equals the dynamic pressure of this velocity. In this concept, the free stream density, or the density on the downstream side of the cloth is used for the computation of the fictitious free stream velocity, V. Figure 2 shows schematically the cloth as a grid, the free stream velocity, V, the pressure differential, Δp, and the average velocity through the cloth called U. The ratio U/V is identified as effective porosity; the nominal porosities presented in Fig 1 are converted to effective porosities and shown in Fig 3.

Looking at the cloth as a porous screen leads to the idea of considering the volumetric flow through the cloth as a function of the openings or orifices and the air resistance of the individual threads, which possibly could be considered as circular cylinders, and a number of attempts have been made to compute the air resistance of a woven sheet in this manner (Refs 9, 10, 11, and 12). However, microscopic pictures (Fig 4) of four frequently used materials indicate that the assumption of a simple cloth geometry may be an oversimplification and the results of a purely analytical treatment in the indicated fashion would probably neglect several significant characteristics. Therefore, it was decided to measure the actual flow rate through the cloth and the results of these experiments will be reviewed in the following.
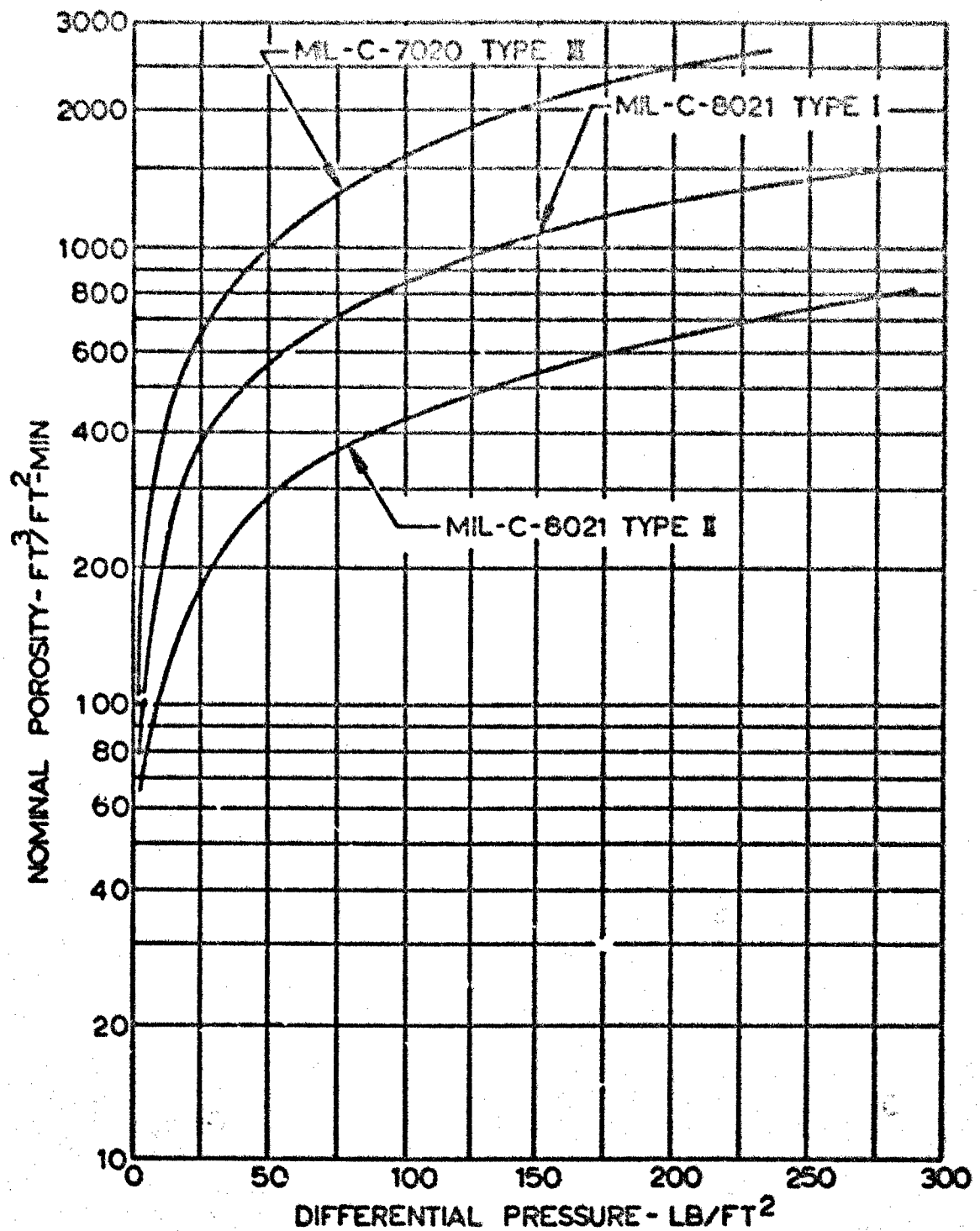
FIG 1. NOMINAL POROSITY OF PARACHUTE MATERIAL VERSUS DIFFERENTIAL PRESSURE
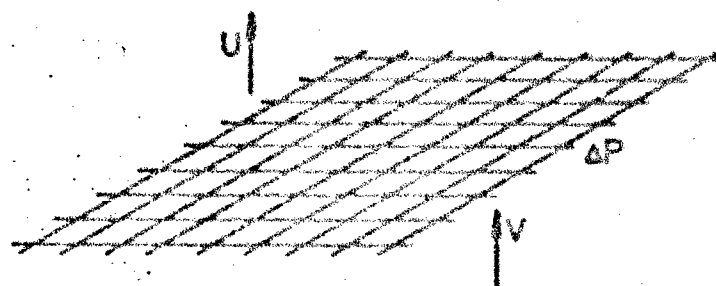
EFFECTIVE POROSITY $C = \dfrac{U}{V}$

WITH $\Delta P = \dfrac{\rho}{2} V^2$, $C = \dfrac{U}{\sqrt{\dfrac{2\Delta P}{\rho}}}$

FIG 2. DERIVATION OF THE TERM 'EFFECTIVE POROSITY'
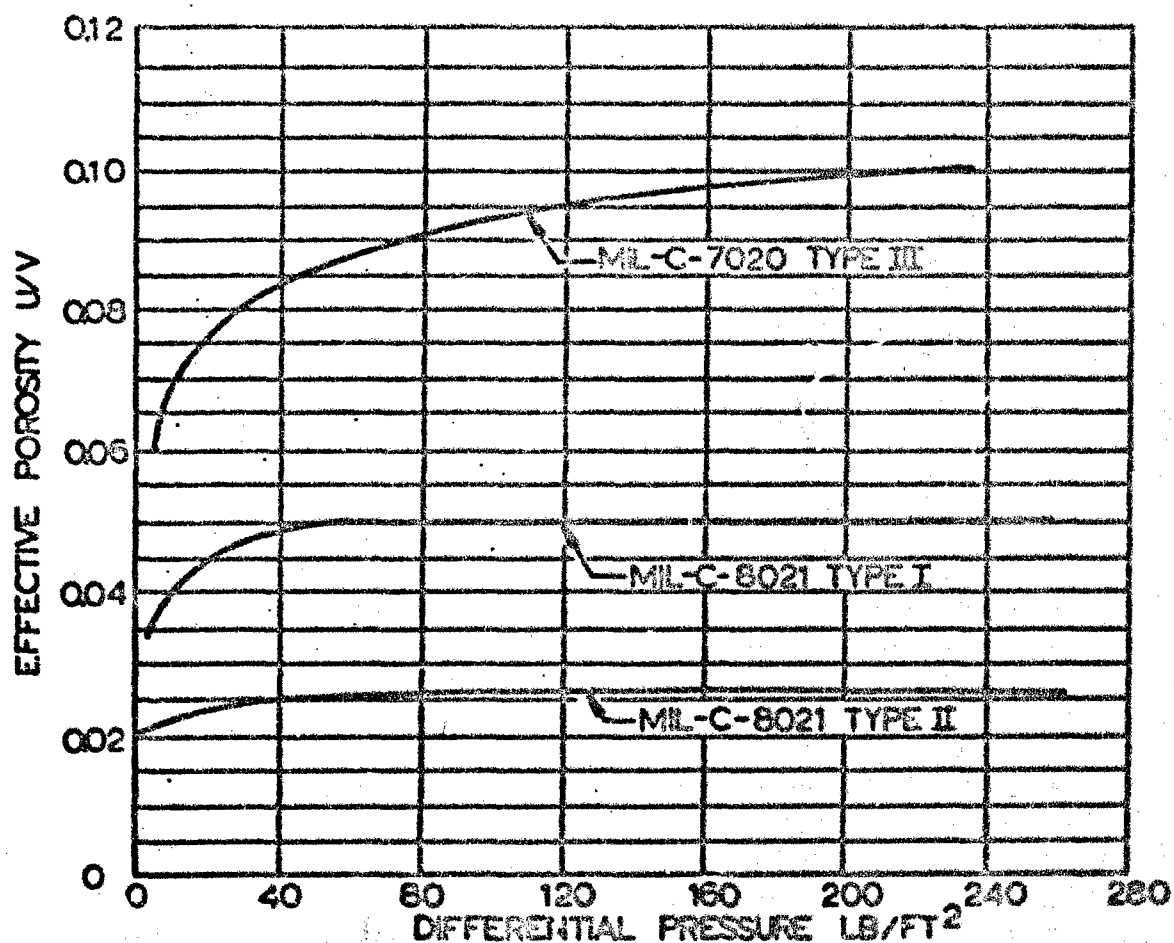
FIG 3. THE EFFECTIVE POROSITY OF PARACHUTE MATERIALS VERSUS DIFFERENTIAL PRESSURE
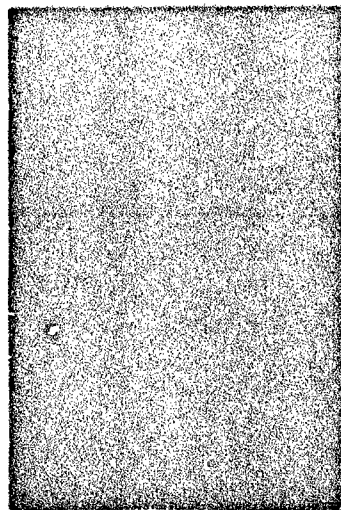
MIL-C-7020 TYPE I, 40 oz/in NYLON, t=0.0032"

MIL-C-7350 TYPE I, 100 oz/in NYLON, t=0.006"

MIL-C-8020 TYPE I, 200 lb/in NYLON, t=0.020"

MIL-C-8020 TYPE II, 300 lb/in NYLON, t=0.024"

FIG 4. MICROSCOPIC PHOTOS OF FOUR GENERALLY USED PARACHUTE MATERIALS (US SPECIFICATIONS)

5

Figure 1 indicates that the flow rate through the cloth increases with the differential pressure. One may assume that this relationship will exist in somewhat monotonic manner, influenced by a Reynolds number effect, until the critical pressure differential is reached at which the velocity through the orifice reaches the speed of sound. A further increase of the differential pressure will then not further increase the air velocity, but a so-called choking effect will occur. Therefore, it appears to be advisable to study the flow in both the incompressible and compressible flow regimes and to interpret the results in view of the classical aspects of Reynolds and Mach numbers.

A further objective of this study is the derivation of a relatively simple relationship between effective porosity and air density, because this may help to explain the increase of opening shock and the change of the stability behavior with altitude.

Considering first incompressible flow, one may assume that the air flows through the fine orifices of a relatively thick cloth somewhat like through a short tube and that the flow is neither completely laminar nor all turbulent. Therefore, an analysis of the two border cases seems to be in order.

For fully developed laminar flow, Hagen-Poiseuille's law provides the following relationship:

$$\Delta p = \frac{128 \mu L Q}{\pi D^4} \tag{1}$$

in which L = length of the tube
$\qquad$ D = diameter of the tube.
With $Q = U \pi D^2/4$, the average velocity in the tube is

$$U = \frac{D^2}{32 \mu L} \Delta p, \tag{2}$$

and the effective porosity may be written

$$C = \frac{U}{V} = \frac{D^2}{32 \mu L} \sqrt{\frac{\rho \Delta p}{2}}, \tag{3}$$

and specifically for sea level density

$$C_0 = \left(\frac{U}{V}\right)_0 = \frac{D^2}{32 \mu_0 L} \sqrt{\frac{\rho_0 \Delta p}{2}}. \tag{3a}$$

6

For the first approximation one may set $\mu_0 = \mu$ and with $\rho/\rho_0 = \sigma$, the effective porosity for any altitude but for the same differential pressure is

$$C = C_0 \sigma^{\frac{1}{2}} \qquad (4)$$

A similar analysis may be made for the assumption of fully developed turbulent flow. With the Blasius formula (Ref 13)

$$\frac{\Delta p}{L} = \frac{\lambda}{D} \cdot \frac{\rho}{2} \cdot U^2 \qquad (5)$$

and

$$\lambda = 0.3164 \left(\frac{U \rho D}{\mu}\right)^{-\frac{1}{4}} \qquad (6)$$

the velocity is

$$U = \left(\frac{2 \Delta p D^{5/4}}{0.3164 L}\right)^{4/7} \left(\mu \rho^3\right)^{-1/7}. \qquad (7)$$

Using $V = (2\Delta p/\rho)^{\frac{1}{2}}$ and the subscript zero for sea level density, the effective porosity C may be written

$$C = C_0 \left(\frac{\Delta p}{\Delta p_0}\right)^{1/14} \left(\frac{\mu_0}{\mu}\right)^{1/7} \left(\frac{\rho}{\rho_0}\right)^{1/14}. \qquad (8)$$

With $\mu_0 = \mu$, and for the same differential pressure, one obtains for fully developed turbulent flow

$$C = C_0 \sigma^{1/14}. \qquad (9)$$

The assumption of both laminar and turbulent flow in the region of incompressibility leads to a relationship of the form

$$C = C_0 \sigma^n, \qquad (10)$$

and it is now one of the objectives of this study to establish experimentally the value of the exponent "n" for various types of parachute material from which one also may conclude if we have laminar, mixed or turbulent flow.

Once the differential pressure is high enough to establish sonic flow, the effective porosity of the cloth

7

will decline with increasing pressure. Therefore, besides
the density ratio, σ, the pressure ratio $\Delta p/\Delta p_{cr}$ shall
be introduced as a basic parameter.

In view of the methods used in the performance
calculations, the experimental study will contain the
velocity U in terms of the volumetric flow on the upstream
or high pressure side of the cloth.

III. MEASUREMENT AND ANALYSIS

In accordance with the preceding analysis, the
effective porosity of one wire screen and four textile
materials frequently used for parachutes were measured by
means of the apparatus shown in Fig 5. The experiments
were made over a density range of σ between 0.1 and 1.0
and a pressure ratio of $\Delta p/\Delta p_{cr}$ between 0.05 and 2.0.
The cloth and wire samples were bonded to a ring with a two
inch internal diameter and then placed in the test section
of the apparatus. The permanent bonding was chosen in order
to avoid slippage with the associated uncertain effective
cloth area. The density ratio, σ, is defined as the ratio
of the density on the downstream side of the porous screen
and the standard sea level density. The wire screen has
been incorporated because one may suspect that the textile
screens change their geometry with the pressure loading
and therefore their observed porosity may reflect not only
Reynolds and Mach number effects, but also consequences
of the elasticity of the cloth. The wire screen would not
have any elasticity effects. In the course of the investi-
gation other wire screens were measured. The results of
these measurements are shown later. These tests did not
serve the purpose of basic analysis but represent merely
quantitative information.

The flow rate in the apparatus shown in Fig 5
was determined by means of calibrated orifice plates or,
when the flow rate was very small, direct indicating flow-
meters were used. Both arrangements are illustrated in
Fig 5. When the orifice method was used, the flow rate
was obtained in a process described in the A.S.M.E. Power
Test Code PTC 195;4-1959. In particular, size and form
of the orifice plates, the arrangement of the pressure
taps and the evaluation of the data points is in accordance
with Fig 1, Chapter 4, and other instructions given in said
document.

FROM HIGH PRESSURE SOURCE

FISCHER-PORTER FLOW METERS

CONTROL VALVES

STILLING CHAMBER

ORIFICE UPSTREAM PRESSURE TAP

ORIFICE DOWNSTREAM PRESSURE TAP

SAMPLE UPSTREAM PRESSURE TAP RING

DOWNSTREAM PRESSURE TAP RING

2 INCH CLOTH SAMPLE

METERING ORIFICE TYPE A.S.M.E. STANDARD REF.

$D = \frac{1}{2}$

$D = 3''$

$D = 2D$

CONTROL VALVE

TO VACUUM SOURCE

9

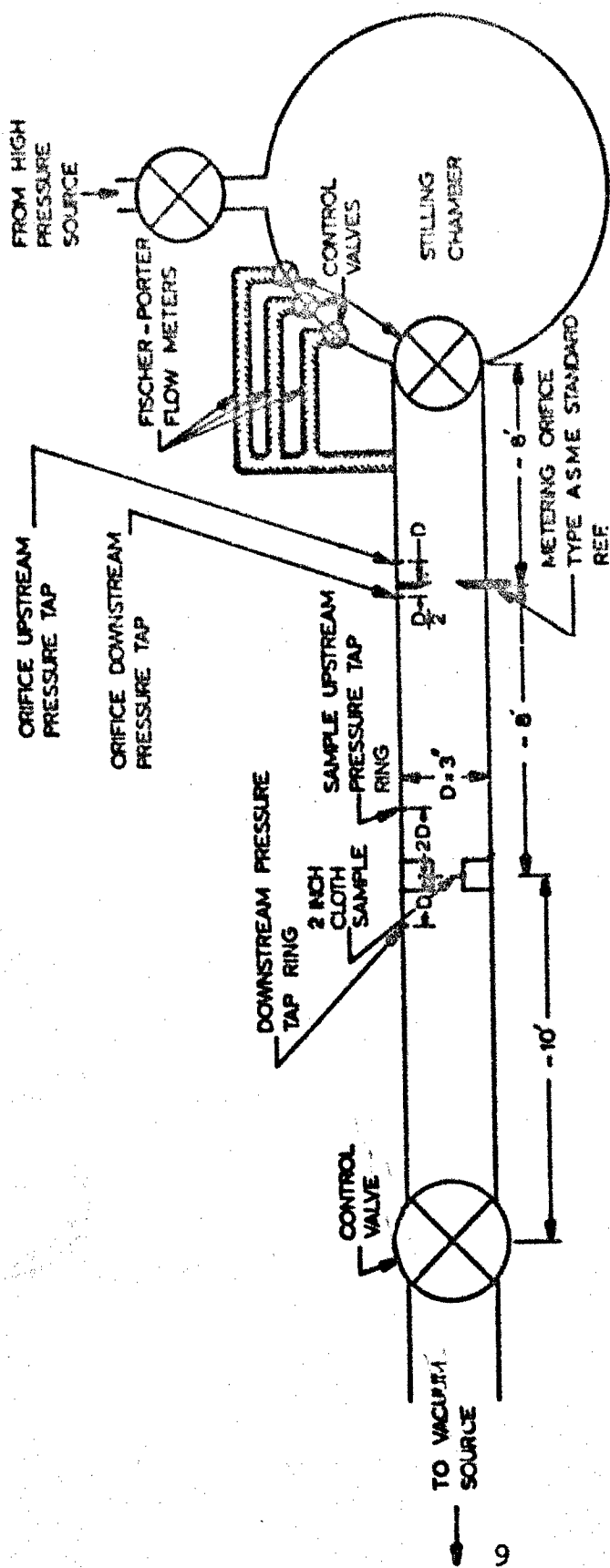FIG 5.   POROSITY MEASURING APPARATUS

Figures 6 through 10 and Tables 1 through 4* show the results of these measurements. It can be seen that the porosity characteristics of the cloth and those of the wire screen are principally identical, and it may be concluded that the most significant characteristics of the recorded effective porosities are consequences of aerodynamic phenomena and not caused by structural deformations.

It is evident that the effective porosity of the wire and cloth screens decreases with decreasing air density. Since for a constant pressure ratio, the density is the prime variable of the governing Reynolds number, it can be concluded that the effective porosity of the screen is a function of the Reynolds number.

The slope of the effective porosity curves versus the differential pressure is in all cases positive up to a certain pressure ratio and then becomes negative. This seems to indicate that the air resistance of the cloth decreases as the Reynolds number increases until compressibility effects become more influential; choking of the flow occurs when sonic speed in the cloth orifices is reached.

Analyzing the limited number of experimental results first in view of Reynolds number effects one may remember the postulation that the effective porosity possibly can be presented as an exponential function on the basis of the density ratio. Therefore, the results shown in Figs 6 through 10 were rearranged in accordance with. Eqn 10 and presented in this form in Figs 11 through 14.

Originally the relationship between effective porosity and density was derived on the basis of identical pressure differential Δp. However, in the following treatment, the pressure ratio, $\Delta p/\Delta p_{cr}$ was used which is also the parameter in the Figs 11 through 14. If the postulated relationships for laminar and turbulent flow are expressed in terms of $\Delta p/\Delta p_{cr}$ and for $\Delta p_{cr} = 0.89 \ P_2$, and also the equation of state is used, one obtains respectively for laminar and turbulent flow relationships

$$ C \ = \ C_o \sigma \tag{11} $$

and

$$ C \ = \ C_o \sigma^{1/7} . \tag{12} $$

---

* Only a limited number of test results have been used. More complete tables will be found in Section V of this report.

TABLE 1

EFFECTIVE POROSITY OF MIL-C-7020B, TYPE I, 40 lb/in NYLON CLOTH

ALL POINTS ARE AVERAGE OF SEVERAL EXPERIMENTAL VALUES

$\frac{\Delta P}{\Delta P_{cr}}$	σ=1.0 C	σ=0.9 C	σ=0.8 C	σ=0.7 C	σ=0.6 C	σ=0.5 C	σ=0.4 C	σ=0.3 C	σ=0.2 C	σ=0.1 C
.03	.052	.050		.047	.044		.039	.033		
.05	.052	.051	.050	.048	.046	.043	.041	.037		.031
.10	.052	.051	.050	.048	.048	.045	.043	.042	.023	.036
.20	.050	.049	.048	.047	.047	.045	.043	.042	.030	.038
.40	.045	.044	.044	.042	.042	.041	.039	.038	.032	.037
.60	.041	.041	.040	.038	.038	.037	.036	.034	.032	.033
.80	.039	.038	.038	.036	.035	.034	.033	.032	.028	.031
1.00	.036		.036	.034	.033	.032	.031	.030	.026	.029
1.50							.028		.022	.024
2.00							.026		.020	

FIG 6. EFFECTIVE POROSITY OF NYLON CLOTH, 40 lb/in, MIL-
C-7020B, TYPE I

12

TABLE 2

EFFECTIVE POROSITY OF MIL-C-7350B, TYPE I, 90 lb/in NYLON CLOTH

ALL POINTS ARE AVERAGE OF SEVERAL EXPERIMENTAL VALUES

$\frac{\Delta P}{\Delta P_{cr}}$	σ=1.0 C	σ=0.9 C	σ=0.8 C	σ=0.7 C	σ=0.6 C	σ=0.5 C	σ=0.4 C	σ=0.3 C	σ=0.2 C	σ=0.1 C
.02	.054	.053	.053	.053				.043		
.05	.055	.054	.054	.054	.054	.053	.047	.046	.035	.021
.10	.054	.054	.054	.053	.053	.052	.048	.045	.041	.032
.20	.051	.051	.051	.050	.050	.049	.047	.035	.031	.031
.40	.046	.045	.045	.044	.044	.043	.042	.040	.038	.04
.60	.041	.041	.040	.040	.039	.038	.037	.036	.035	.032
.80	.038	.037	.037	.036	.036	.035	.034	.033	.032	.020
1.00	.035	.035	.034	.033	.033	.032	.032	.031	.029	.027
1.50	.030	.030	.029	.029	.028	.028	.028	.026	.025	.031
2.00							.025	.024	.023	.021

FIG 7 EFFECTIVE POROSITY OF NYLON CLOTH, 90 lb/in, MIL-
C-7350B, TYPE I

14

TABLE 3

EFFECTIVE POROSITY OF MIL-C-8021A, TYPE I, 200 lb/in NYLON CLOTH

ALL POINTS ARE AVERAGE OF SEVERAL EXPERIMENTAL VALUES

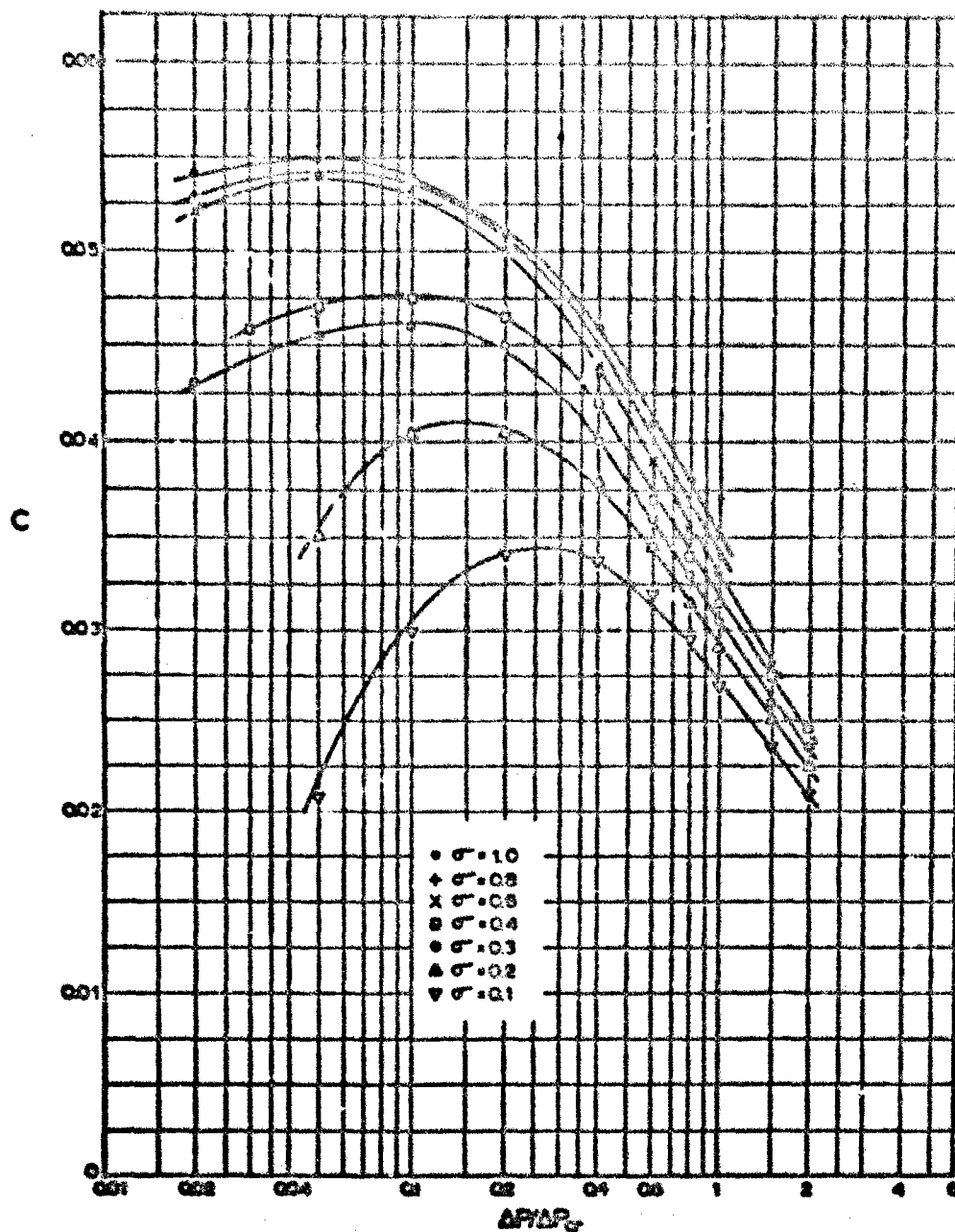| $\frac{\Delta P}{\sqrt{\Delta P_{cr}}}$	σ=.10 C	σ=.09 C	σ=.08 C	σ=.07 C	σ=.06 C	σ=.05 C	σ=.04 C	σ=.03 C	σ=.02 C	σ=.01 C
.02				.016	.015					
.05				.019	.018	.016	.015	.012		
.10	.023	.023	.021	.020	.019	.018	.017	.014	.012	
.20	.023	.023	.022	.021	.020	.019	.018	.016	.013	.010
.40	.021	.021	.021	.020	.020	.019	.018	.017	.014	.012
.60	.020	.020	.019	.019	.019	.018	.017	.016	.014	.012
.80	.019	.019	.018	.018	.018	.017	.016	.015	.014	.012
1.00	.018	.018	.017	.017	.017	.016	.015	.014	.013	.012
1.50	.016	.016	.015	.015	.014	.014	.014	.013	.012	.011
2.00	.014	.014	.014	.013	.013	.013	.013	.012	.011	.010

FIG 8. EFFECTIVE POROSITY OF NYLON CLOTH, 200 lb/in, MIL-
C-8021A, TYPE I

16

TABLE 4

EFFECTIVE POROSITY OF MIL-C-8021A, TYPE II, 300 lb/in NYLON CLOTH

ALL POINTS ARE AVERAGE OF SEVERAL EXPERIMENTAL VALUES

σ=0.1 ΔP/ΔPcr	C	σ=0.2 ΔP/ΔPcr	C	σ=0.3 ΔP/ΔPcr	C	σ=0.4 ΔP/ΔPcr	C	σ=0.5 ΔP/ΔPcr	C	σ=0.6 ΔP/ΔPcr	C	σ=0.7 ΔP/ΔPcr	C	σ=0.8 ΔP/ΔPcr	C	σ=0.9 ΔP/ΔPcr	C	σ=1.0 ΔP/ΔPcr	C
.10	.016	.10	.021	.10	.022	.10	.023	.10	.027	.10	.026	.10	.027	.10	.028	.10	.028	.10	.029
.20	.018	.20	.022	.20	.023	.20	.023	.20	.026	.20	.026	.20	.027	.20	.027	.20	.028	.20	.028
.40	.018	.40	.021	.40	.021	.40	.022	.40	.022	.40	.024	.40	.024	.40	.025	.40	.026	.40	.026
.60	.017	.60	.019	.60	.020	.60	.021	.60	.021	.60	.022	.60	.022	.60	.023	.60	.024	.60	.024
.80	.016	.80	.018	.80	.018	.80	.019	.80	.020	.80	.020	.80	.021	.80	.021	.80	.022	.80	.022
1.00	.015	1.00	.017	1.00	.017	1.00	.018	1.00	.019	1.00	.019	1.00	.019	1.00	.020	1.00	.020	1.00	.021
1.50	.014	1.50	.015	1.50	.015	1.50	.015	1.50	.015	1.50	.017	1.50	.017	1.50	.017	1.50	.018	1.50	.018
2.00	.012	2.00	.013	2.00	.013	2.00	.013	2.00	.015	2.00	.015	2.00	.015	2.00	.015	2.00	.015	2.00	.015

FIG 9. EFFECTIVE POROSITY OF NYLON CLOTH, 300 lb/in, MIL-
C-8021A, TYPE II

18

C

$\Delta P / \Delta P_{cr}$

Legend:
- $\bullet$ $\sigma = 0.648$
- $+$ $\sigma = 0.519$
- $\times$ $\sigma = 0.418$
- $\square$ $\sigma = 0.224$
- $\circ$ $\sigma = 0.0775$
- $\triangle$ $\sigma = 0.0207$

FIG 10. EFFECTIVE POROSITY VERSUS PRESSURE RATIO FOR 30×40 MESH STRANDED WEAVE WIRE SCREEN

19

FIG 11. NONDIMENSIONAL EFFECTIVE POROSITY VERSUS DENSITY RATIO FOR MIL-C-7020III, TYPE I, 40 lb/h NYLON CLOTH

FIG 12   NONDIMENSIONAL EFFECTIVE POROSITY VERSUS DENSITY RATIO FOR MIL-C-7350B, TYPE I, 90 b/in
NYLON CLOTH
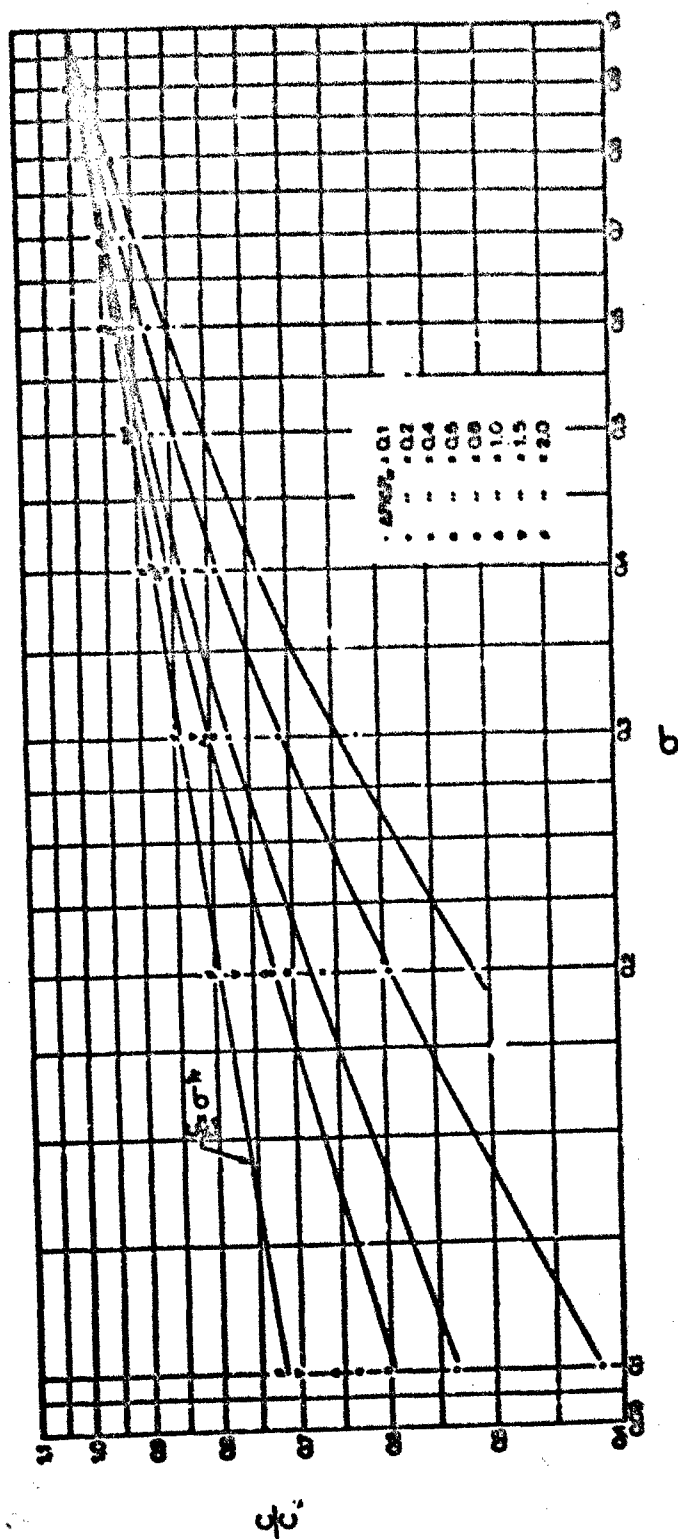
FIG 13. NONDIMENSIONAL EFFECTIVE POROSITY VERSUS DENSITY RATIO FOR MIL-C-8021A TYPE I, 200 t/h
NYLON CLOTH

22
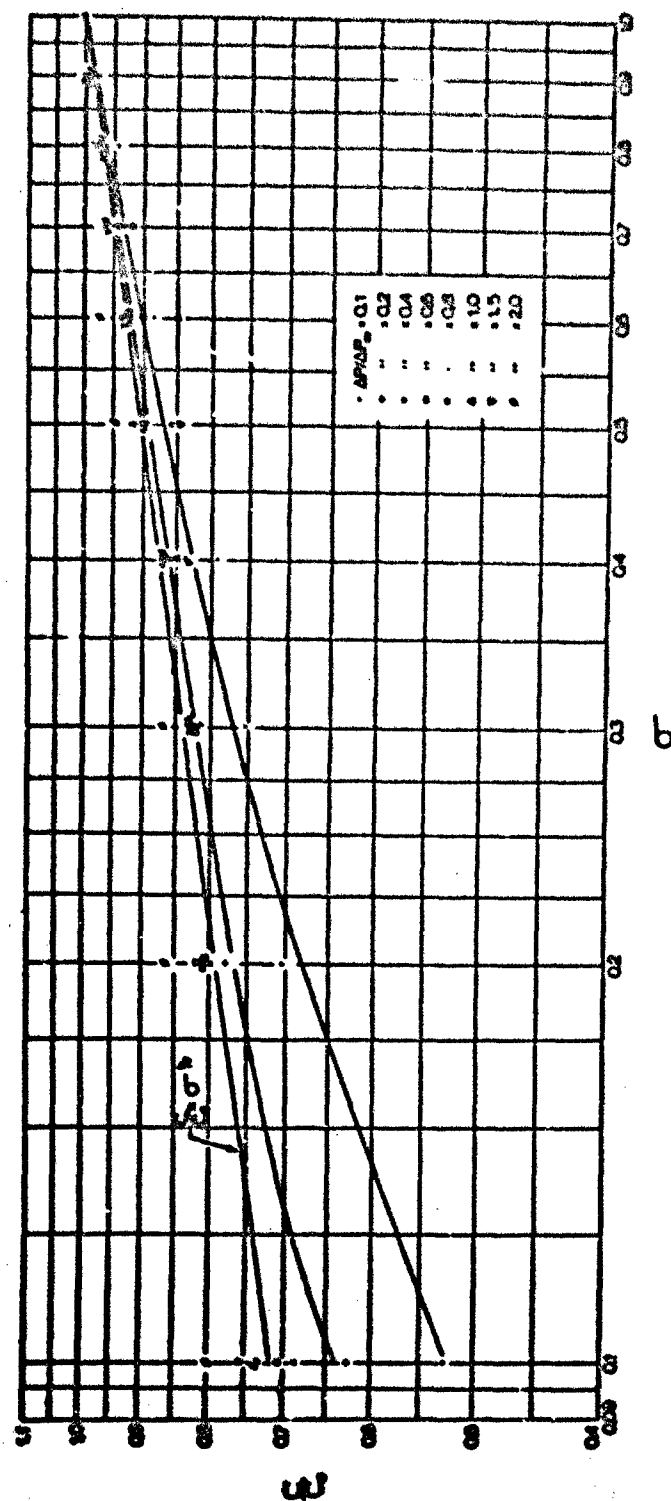
FIG 14 NONDIMENSIONAL EFFECTIVE POROSITY VERSUS DENSITY RATIO FOR MIL-C-8021A, TYPE I, 300 lb/in NYLON CLOTH

Reviewing the results shown in Figs 11 through 14, one observes that the results of many experiments seem to follow Eqn 12 almost perfectly which would indicate fully developed turbulent flow. The minimum pressure at which this occurs varies with the thickness and the type of weave of the cloth.

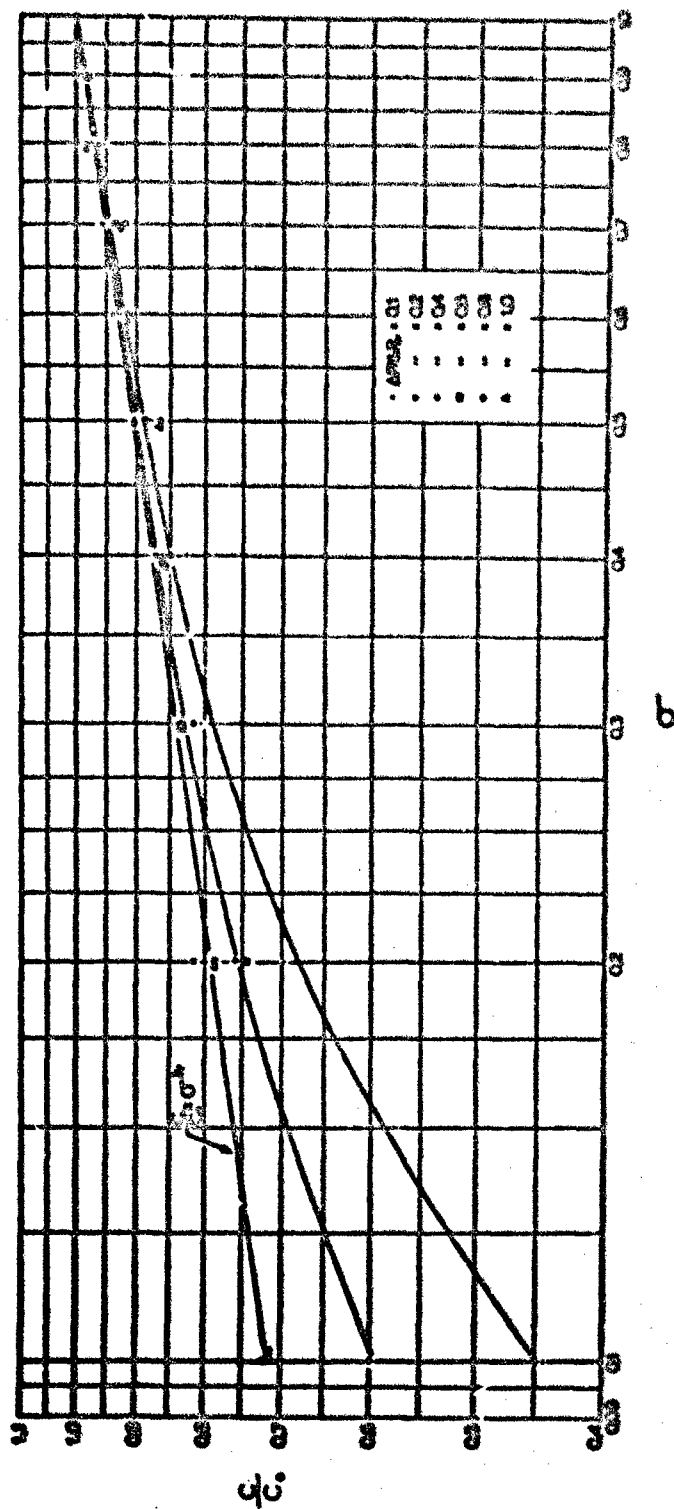All cloths under investigation indicate an exponent larger than 1/7 for relatively small density and low pressure ratios. In particular, the lightest and thinnest cloth with a tensile strength of 40 lb per inch approaches for very low density and smaller differential pressures the relationship shown in Eqn 11. This indicates that for this type of cloth and under these flow conditions, the flow through this cloth is nearly laminar.

In general, the experiments confirm the original assumption that the effective porosity of these porous cloths is a function of the Reynolds number. The practical aspect of these experiments is the fact that for the same differential pressure or for the same pressure ratio, the effective porosity of the woven cloth decreases with decreasing density.

The exponent in Eqn 10 signifies the character of the flow through the cloth orifices, and for further analysis it appears to be useful to plot the density exponent "n", versus the Reynolds number of the related flow condition.

A meaningful Reynolds number can be established for a rectangular stream tube which approaches the cloth from the free stream and which then passes through the orifice of the cloth. The width of this stream tube before passing through the orifice is the characteristic length, L, and can be found from the number of threads per unit length of the cloth.

In view of the definition of the effective porosity, the Reynolds number of the stream tube is

$$R_e = \frac{LCV\rho_1}{\mu} .$$
(13)

Since all density references in this study are made in relationship to the downstream conditions, one may introduce

$$\rho_1 = \rho_2 \frac{P_1}{P_2} \cdot \frac{T_2}{T_1}$$

Experimentally it was found that $T_1 \cong T_2$ and with $P_1 = P_2(1 + 0.89 \Delta p / \Delta p_{cr})$ and $\rho_2 = \rho_0 \sigma$, the upstream density

24

amounts to

$$\rho_1 = \rho_0 \sigma (1 + 0.89 \, \Delta p / \Delta p_{cr}). \tag{14}$$

By definition

$$
\begin{aligned}
V &= \left(\frac{2 \, \Delta p}{\rho_2} \right)^{\frac{1}{2}} \\[6pt]
&= \left(\frac{2(P_1 - P_2) R T_2}{P_2} \right)^{\frac{1}{2}} \\[6pt]
&= \left(1.78 \, \frac{\Delta p}{\Delta p_{cr}} \, R T_2 \right)^{\frac{1}{2}}. \tag{15}
\end{aligned}
$$

Again, with $T_1 \cong T_2$, and combining Eqns 13, 14, and 15, the Reynolds number of the stream tube amounts to

$$R_e = \frac{L C \rho_0 \sigma}{\mu} \left(1 + 0.89 \, \frac{\Delta p}{\Delta p_{cr}} \right) \cdot \left(1.78 \, \frac{\Delta p}{\Delta p_{cr}} \, R T_2 \right)^{\frac{1}{2}}. \tag{16}$$

The Reynolds numbers of the experiments, derived in accordance with Eqn 16, are now combined with the density exponents of Figs 11 through 14 as shown in Figs 15 through 18. It can be seen that all four fabrics apparently have fully developed turbulent flow at Reynolds numbers larger than 200. The region of transition is obviously between Reynolds numbers of 100 and 200. The lightest and thinnest cloth approaches laminar flow at a Reynolds number of approximately 10 whereas the heavier materials indicate a mixed flow for the same Reynolds number. The thickest and heaviest cloth, 300 lb per inch tensile strength, has apparently the highest degree of turbulence and the lowest Reynolds number at which transition to full turbulence occurs.
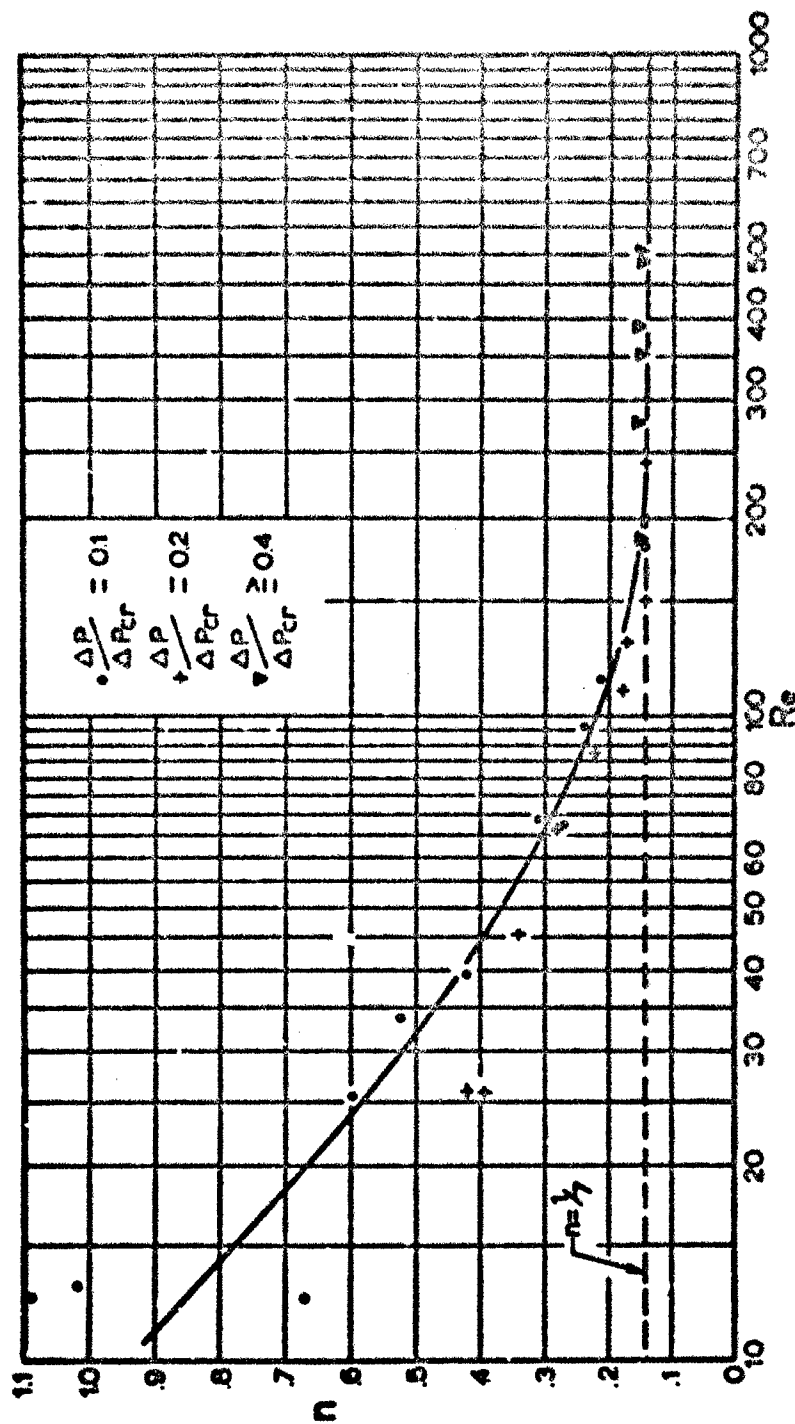
FIG 15 DENSITY EXPONENT VERSUS REYNOLDS NO. FOR MIL-C-7020B, TYPE I, 40 lb/IN NYLON CLOTH
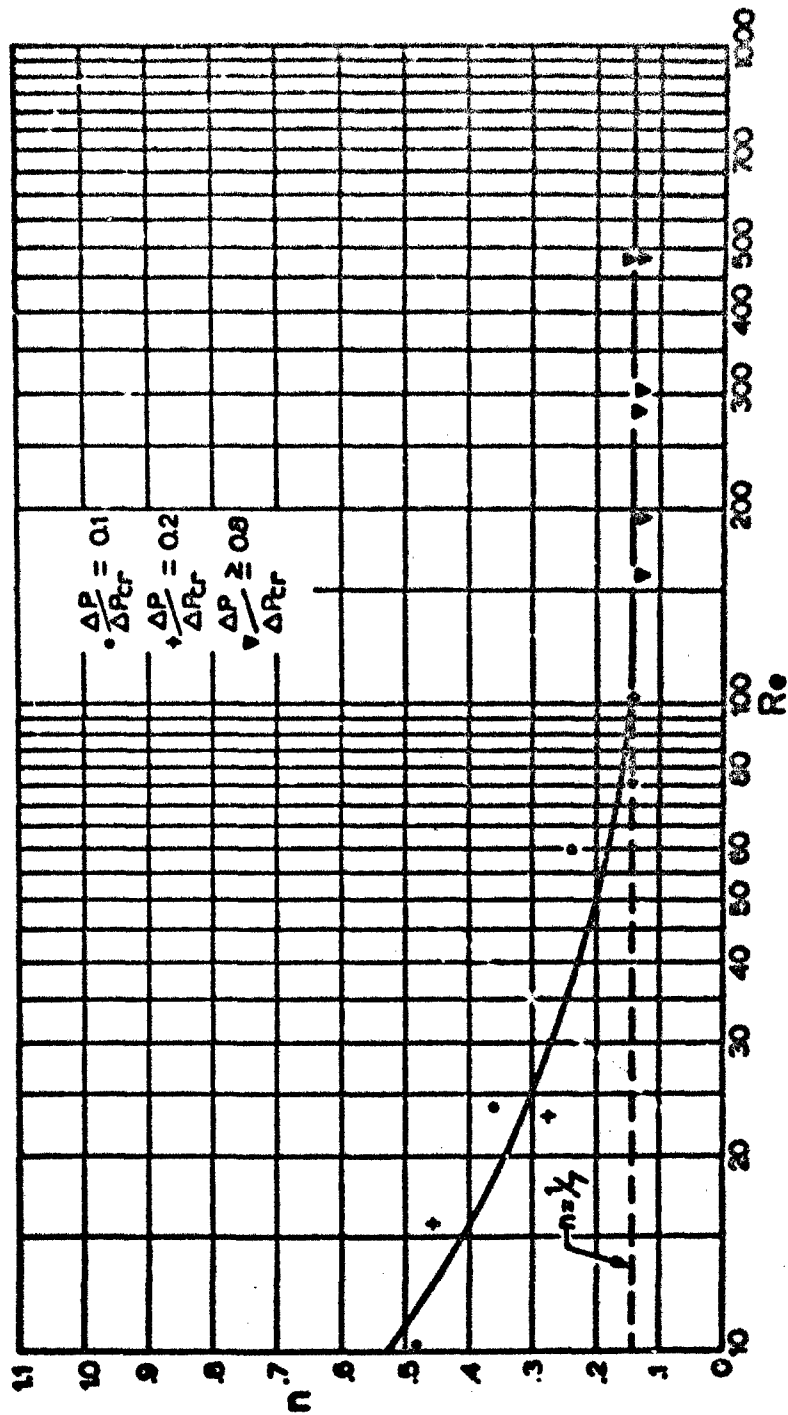
FIG 16 DENSITY EXPONENT VERSUS REYNOLDS NO. FOR MIL-C-7350B, TYPE I 90 lb/in NYLON CLOTH
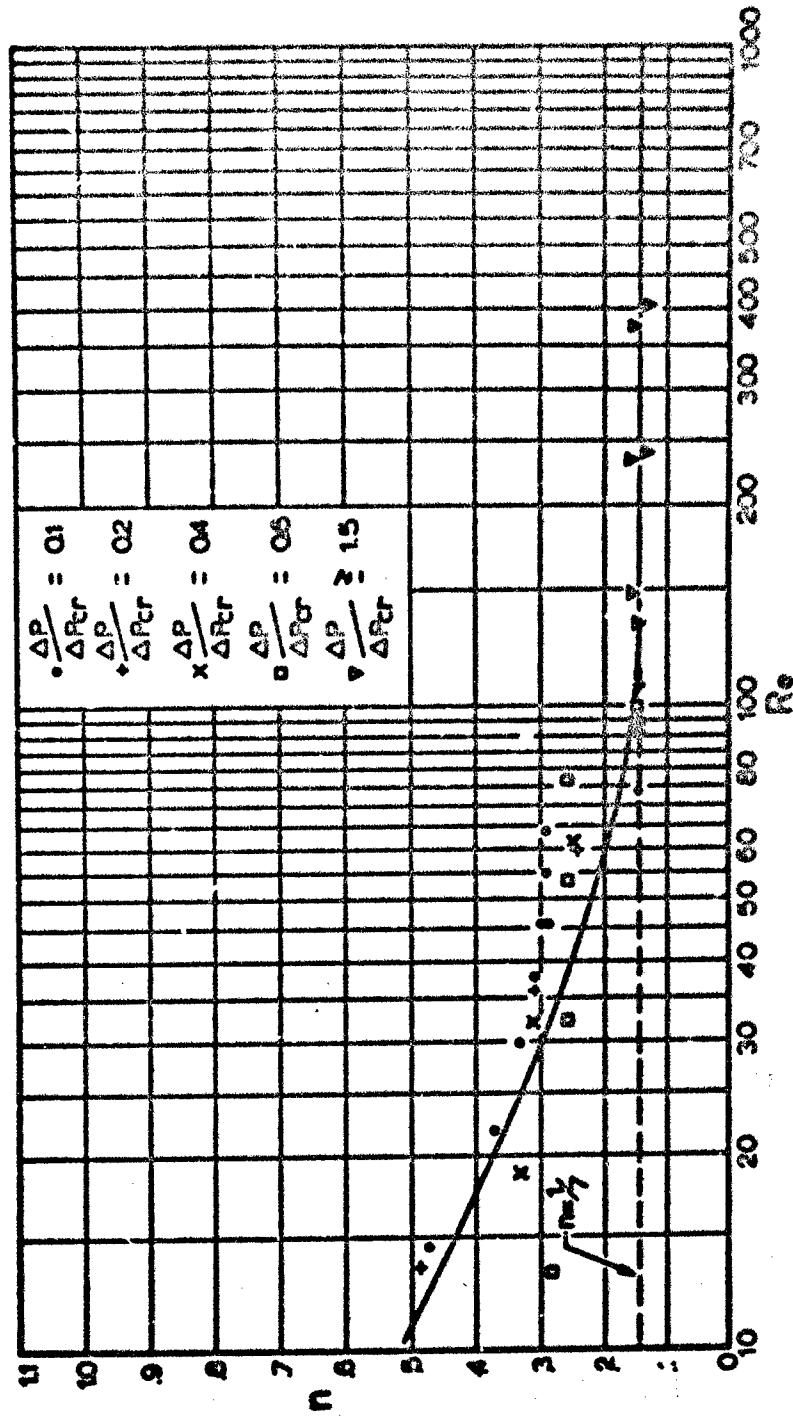
FIG 17 DENSITY EXPONENT VERSUS REYNOLDS NO. FOR MIL-C-8021A, TYPE I, 200 lb/in NYLON CLOTH
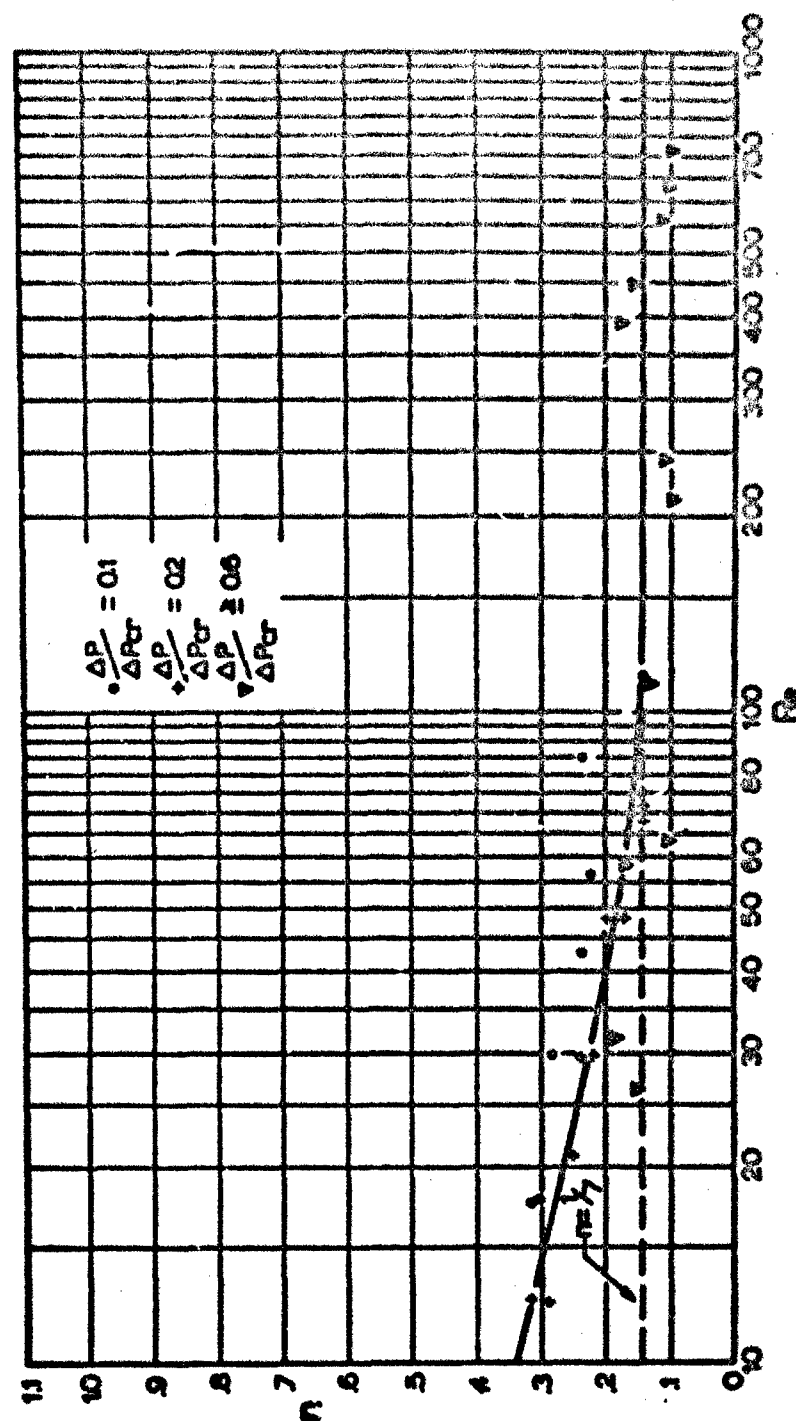
FIG 18 DENSITY EXPONENT VERSUS REYNOLDS NO. FOR MIL-C-8021A,
TYPE II, 300 lb/IN NYLON CLOTH

IV. CALCULATION OF THE EFFECTIVE POROSITY

In view of the surprising regularities between effective porosity and Reynolds and Mach numbers, one is indeed tempted to calculate the flow of air through the cloth by a somewhat conventional method.

Utilizing again the stream tube concept, one orifice in the cloth may be considered to be a nozzle with a particular discharge coefficient. For mechanical nozzles, such discharge coefficients are known, as for example, in Ref 14, from which Fig 19 is taken.

With the energy equation, continuity condition, and adiabatic expansion one has for the flow velocity in a jet the equation (Ref 15):

$$U = \frac{A_2}{A_1} \left(\frac{P_2}{P_1}\right)^{1/\gamma} \left(\frac{2\frac{\gamma}{\gamma-1} \cdot \frac{P_1}{\rho_1} \cdot \left[1 - \left(\frac{P_2}{P_1}\right)^{\frac{\gamma-1}{\gamma}}\right]}{1 - \left(\frac{A_2}{A_1}\right)^2 \left(\frac{P_2}{P_1}\right)^{2/\gamma}} \right)^{\frac{1}{2}} \qquad (17)$$

in which A_2/A_1 represents the contraction ratio of the stream tube.

Microscopic pictures show that the contraction ratio A_2/A_1 is in the order of 0.07, and since $P_1 > P_2$, Eqn 17 can be simplified to:

$$U = \frac{A_2}{A_1} \left(\frac{P_2}{P_1}\right)^{1/\gamma} \left(2\frac{\gamma}{\gamma-1} \cdot \frac{P_1}{\rho_1} \cdot \left[1 - \left(\frac{P_2}{P_1}\right)^{\frac{\gamma-1}{\gamma}}\right] \right)^{\frac{1}{2}} \qquad (17a)$$

Introducing the equation of state and rearranging Eqn 17a provides:

$$U = \frac{A_2}{A_1} \cdot \frac{P_2}{P_1} \left(2 RT_1 \frac{\gamma}{\gamma-1} \left(\frac{P_1}{P_2}\right)^{\frac{\gamma-1}{\gamma}} \left[\left(\frac{P_1}{P_2}\right)^{\frac{\gamma-1}{\gamma}} - 1\right] \right)^{\frac{1}{2}} \qquad (18)$$

If the critical pressure ratio between the two sides of the cloth is reached, $P_2/P_1 = 0.528$, sonic velocity exists in the orifices or in the throat of the assumed

nozzle. For this condition one has (Ref 15):

$$\frac{P_{thr}}{P_\infty} = \left(\frac{2}{\gamma+1}\right)^{\frac{\gamma}{\gamma-1}} . \tag{19}$$

Because of $A_2/A_1 \ll 1$, $P_1 \approx P_\infty$, and P_2 replaced by P_{thr}, Eqn 17a provides

$$U = \frac{A_2}{A_1} \left[\gamma \left(\frac{2}{\gamma+1}\right)^{\frac{\gamma+1}{\gamma-1}} \frac{P_1}{\rho_1} \right]^{\frac{1}{2}} . \tag{20}$$

Equations 18 and 20 can now be used in the expression for the effective porosity, which is

$$C = \frac{U}{V}$$

with

$$V = \left[\frac{2(P_1 - P_2)}{\rho_2}\right]^{\frac{1}{2}} . \tag{21}$$

Furthermore, the experiments indicated $T_1 \approx T_2$, and introducing for viscous flow the discharge coefficient, K, Ref 14, Fig 19, the effective porosity for the subcritical case follows from Eqns 18 and 21 with the equation of state for

$$\rho_2 = \frac{P_2}{RT_2} ,$$

$$C = K \frac{A_2}{A_1} \frac{P_2}{P_1} \left(\frac{\frac{\gamma}{\gamma-1} \left|\frac{P_1}{P_2}\right|^{\frac{\gamma-1}{\gamma}} \left[\left(\frac{P_1}{P_2}\right)^{\frac{\gamma-1}{\gamma}} - 1 \right]}{\frac{P_1}{P_2} - 1} \right)^{\frac{1}{2}} . \tag{22}$$

For the critical and supercritical case, Eqn 20 and 21 provide

$$C = K \frac{A_2}{A_1} \left(\frac{\frac{\gamma}{2} \left[\frac{2}{\gamma+1}\right]^{\frac{\gamma+1}{\gamma-1}}}{\frac{P_1}{P_2} - 1} \right)^{\frac{1}{2}} . \tag{23}$$

31
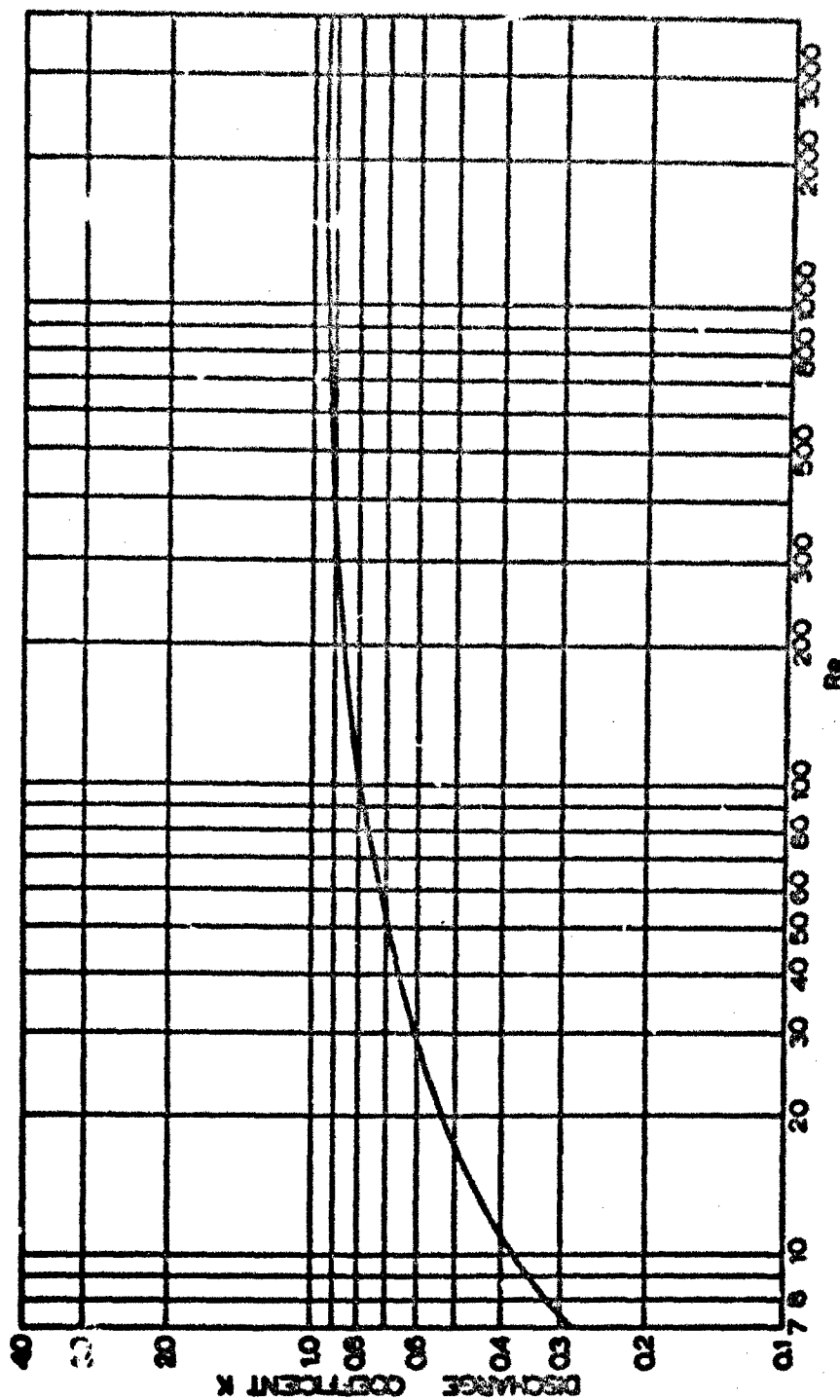
FIG 19. NOZZLE DISCHARGE COEFFICIENT *
*FROM REFERENCE 14

32

These equations can now be written in terms of $\Delta p / \Delta p_{cr}$ and one obtains for

$$\frac{P_1}{P_2} = 0.893 \frac{\Delta p}{\Delta p_{cr}} + 1$$

which allows one to write Eqns 22 and 23 in the following form:

$$C = \frac{K \frac{A_2}{A_1}}{0.893 \frac{\Delta p}{\Delta p_{cr}} + 1} \left(\frac{1}{0.893 \frac{\Delta p}{\Delta p_{cr}}} \left(\frac{\gamma}{\gamma - 1} \right) \right. \cdot$$

$$\left. \cdot \left[0.893 \frac{\Delta p}{\Delta p_{cr}} + 1 \right]^{\frac{\gamma - 1}{\gamma}} \left[\left(0.893 \frac{\Delta p}{\Delta p_{cr}} + 1 \right)^{\frac{\gamma - 1}{\gamma}} - 1 \right] \right)^{\frac{1}{2}}, \quad (22a)$$

$$C = K \frac{A_2}{A_1} \left[\frac{\frac{\gamma}{2} \left(\frac{2}{\gamma + 1} \right)^{\frac{\gamma + 1}{\gamma - 1}}}{0.893 \frac{\Delta p}{\Delta p_{cr}}} \right]^{\frac{1}{2}} . \quad (23a)$$

The equations above, combined with the Reynolds number from Eqn 16 and the discharge coefficient from Fig 19 provide now a certain basis to calculate the effective porosity under a number of idealizing assumptions. These assumptions are a certain regularity of the cloth porosity, the knowledge of the actual geometric porosity of the cloth, and the identity of the discharge coefficients of the cloth orifices and a mechanical nozzle. Of course, these conditions are not exactly fulfilled. Furthermore, the flow through the cloth under the condition of very small Reynolds numbers may fall in the slip and transitional flow regime connected with a drastic change of specific air resistance. These effects are not considered in the present analysis.

Figure 20 is a comparison of experimental and calculated results. The results fit well enough to allow the statement, that the presented treatment of cloth porosity appears to come close to the actual mechanics of the flow phenomena. Appreciable deviations occur where one would suspect a Knudsen number influence, the study of which, however, is beyond the scope of this investigation.

33
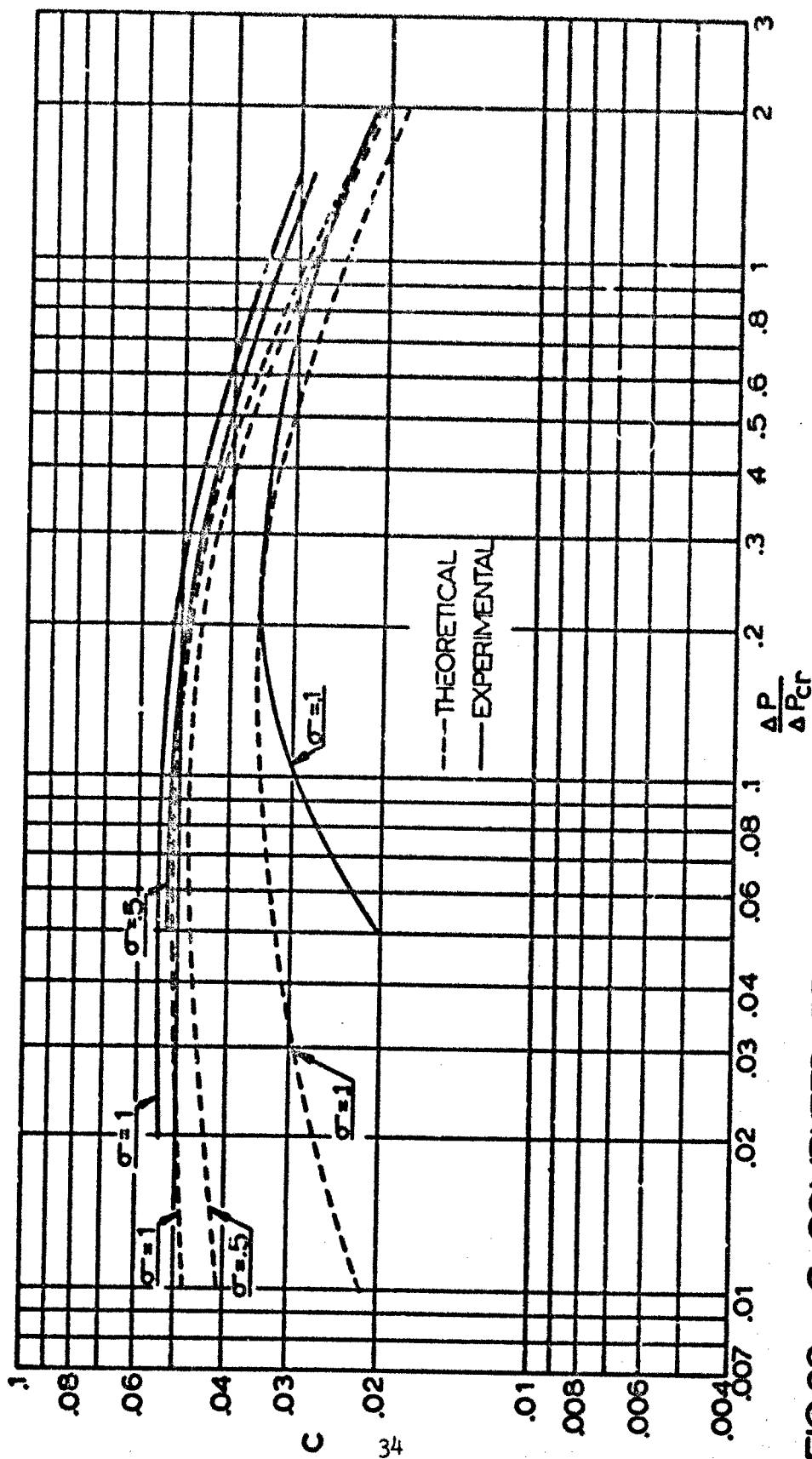
FIG 20. C COMPUTED FROM THE ISENTROPIC FLOW EQUATION AND EMPIRICAL DISCHARGE COEFFICIENT; AND EXPERIMENTAL VALUES OF C FOR 90 lb/in CLOTH

34

V. EXPERIMENTAL RESULTS FOR PARACHUTE
PERFORMANCE CALCULATIONS

The principal objective in the preceding analysis was the study of the mechanics of the flow through the woven textile screens. For parachute performance calculations some directly applicable values are probably most welcome. Therefore, an independent series of experiments were conducted in which numerous cloth samples were examined and reliable average values established. The results of these tests are presented in Figs 21 through 26 and Tables 5 through 10.

It can be seen that the experiments were extended 1.to the regimes of very low pressure and density ratios which occur during parachute operations at relatively low speed and at low as well as at high altitudes, including the conditions of steady state descent.

Furthermore, a very porous Perlon screen has been incorporated, which is used for the fabrication of a particular type of supersonic parachute. Also a number of wire screens were investigated. The respective results are shown in the Appendix. The measurements of these screens may not have a direct bearing on a study of screen porosities in view of parachute technology, but they may be considered to be related data.

All investigated samples show the principal porosity characteristics as discussed in the preceding paragraphs, and these additional tests may be considered as a further proof of the general conclusions derived in the preceding flow analysis.

VI. SUMMARY

The investigation has shown that the effective porosity of woven sheets can be calculated in the right order of magnitude, and that its characteristics follow the general aerodynamic principles related to Reynolds and Mach numbers. In particular the investigation has shown that under otherwise similar circumstances, the effective porosity decreases with the air density, which explains at least in part the variation of the parachute performance characteristics with altitude.

TABLE 5

EFFECTIVE POROSITY OF 40 lb/in NYLON CLOTH MIL-C-7020B, TYPE I, AT VARIOUS PRESSURE AND DENSITY RATIOS

ALL POINTS ARE AVERAGE OF SEVERAL EXPERIMENTAL VALUES

| $\Delta p/\bar{\sigma}$ \ σ	0.05	0.1	0.2	0.3	0.4	0.5	0.6	0.7	0.8	0.9	1.0
2.0000	.0212	.0244	.0269	.0294	.0319		.0429	.0448	.0469	.0489	.0509
1.0000	.0253	.0315	.0339	.0268	.0389	.0412	.0445	.0460	.0475	.0495	.0505
0.7000	.0275	.0340	.0358	.0291	.0411	.0420	.0435	.0465	.0470	.0492	.0512
0.3000	.0289	.0378	.0414	.0446	.0464	.0475	.0522	.0534	.0544	.0508	.0535
0.1000	.0233	.0343	.0425	.0460	.0481	.0511	.0517	.0528	.0535	.0548	.0535
0.0700	.0219	.0311	.0405	.0449	.0471	.0508	.0478	.0491	.0459	.0510	.0479
0.0300	.0138	.0249	.0343	.0399	.0423	.0465	.0418	.0425	.0425	.0448	.0470
0.0100		.0162	.0250	.0221	.0351	.0387	.0382	.0393	.0412	.0427	.0446
0.0070		.0139	.0218	.0293	.0330	.0359	.0331	.0348	.0362	.0372	.0367
0.0030		.0039	.0151	.0218	.0265	.0299	.0235	.0258	.0279	.0304	.0310
0.0010				.0136	.0171	.0200	.0199	.0226	.0246	.0259	.0279
0.0007				.0117	.0146	.0174	.0154	.0178	.0198	.0213	.0213
0.0004					.0109	.0131		.0125	.0141	.0159	.0175
0.0002											

36
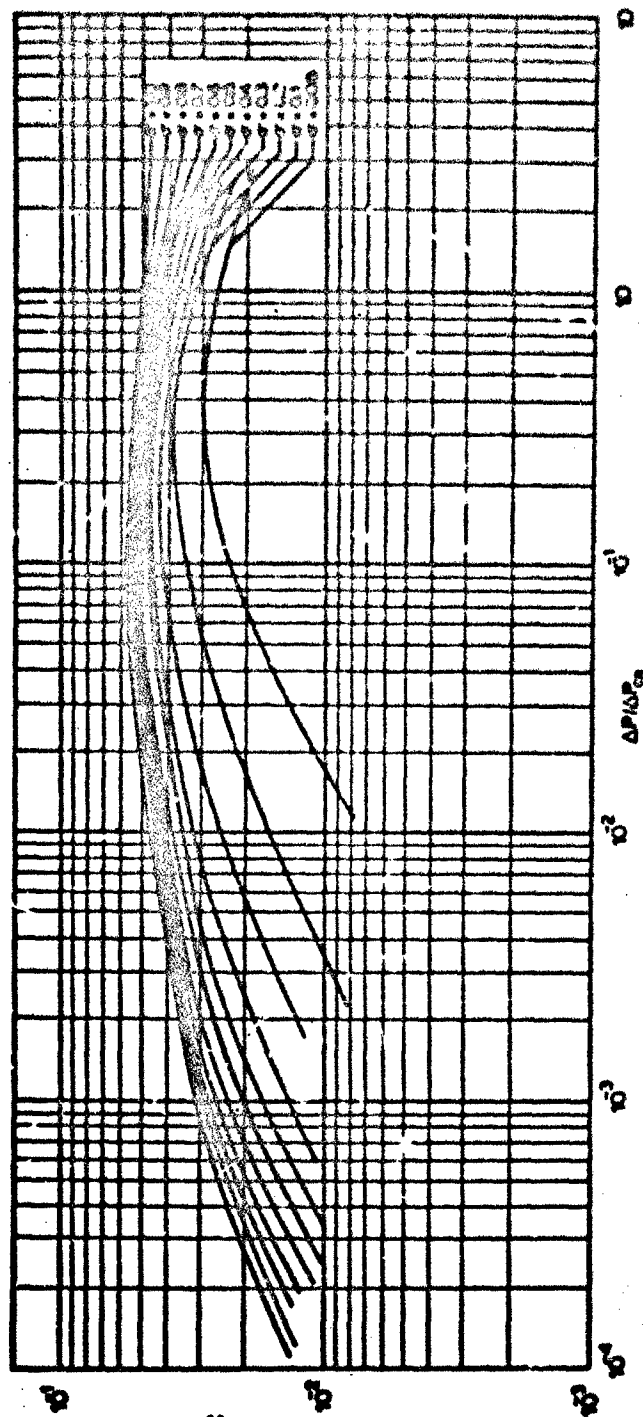
FIG 21 EFFECTIVE POROSITY VERSUS PRESSURE RATIO FOR MIL-C-7020A TYPE I, 4.0 oz/yd NYLON CLOTH

TABLE 6

EFFECTIVE POROSITY OF 90 lb/in NYLON CLOTH MIL-C-7350B, TYPE I, AT VARIOUS PRESSURE AND DENSITY RATIOS

ALL POINTS ARE AVERAGE OF SEVERAL EXPERIMENTAL VALUES

| $\frac{\Delta P_2}{\Delta P_1}$ \\ σ	0.05	0.1	0.2	0.3	0.4	0.5	0.6	0.7	0.8	0.9	1.0
2.0000		.0239	.0274	.0300	.0311	.0321	.0344	.0357	.0369	.0384	.0384
1.0000		.0295	.0334	.0361	.0382	.0398	.0410	.0432	.0438	.0454	.0454
0.7000	.0220	.0322	.0361	.0389	.0416	.0431	.0445	.0464	.0467	.0487	.0487
0.3000	.0295	.0371	.0421	.0451	.0487	.0502	.0522	.0530	.0537	.0555	.0555
0.1000	.0303	.0359	.0437	.0486	.0520	.0538	.0562	.0571	.0585	.0585	.0585
0.0700	.0291	.0346	.0430	.0485	.0519	.0539	.0560	.0570	.0589	.0589	.0589
0.0300	.0230	.0299	.0399	.0468	.0494	.0510	.0525	.0539	.0560	.0562	.054
0.0100		.0220	.0326	.0401	.0428	.0448	.0459	.0476	.0499	.0512	.0524
0.0070		.0191	.0297	.0371	.0398	.0425	.0437	.0455	.0475	.0498	.0508
0.0030		.0129	.0228	.0294	.0320	.0359	.0386	.0414	.0426	.0451	.0469
0.0010			.0150	.0191	.0232	.0280	.0319	.0341	.0355	.0372	.0392
0.0007			.0131	.0159	.0219	.0258	.0291	.0315	.0331	.0345	.0365
0.0004				.0114	.0175	.0224	.0246	.0270	.0290	.0310	.0324
0.0002					.0139	.0169	.0197	.0221	.0239	.0255	.0273
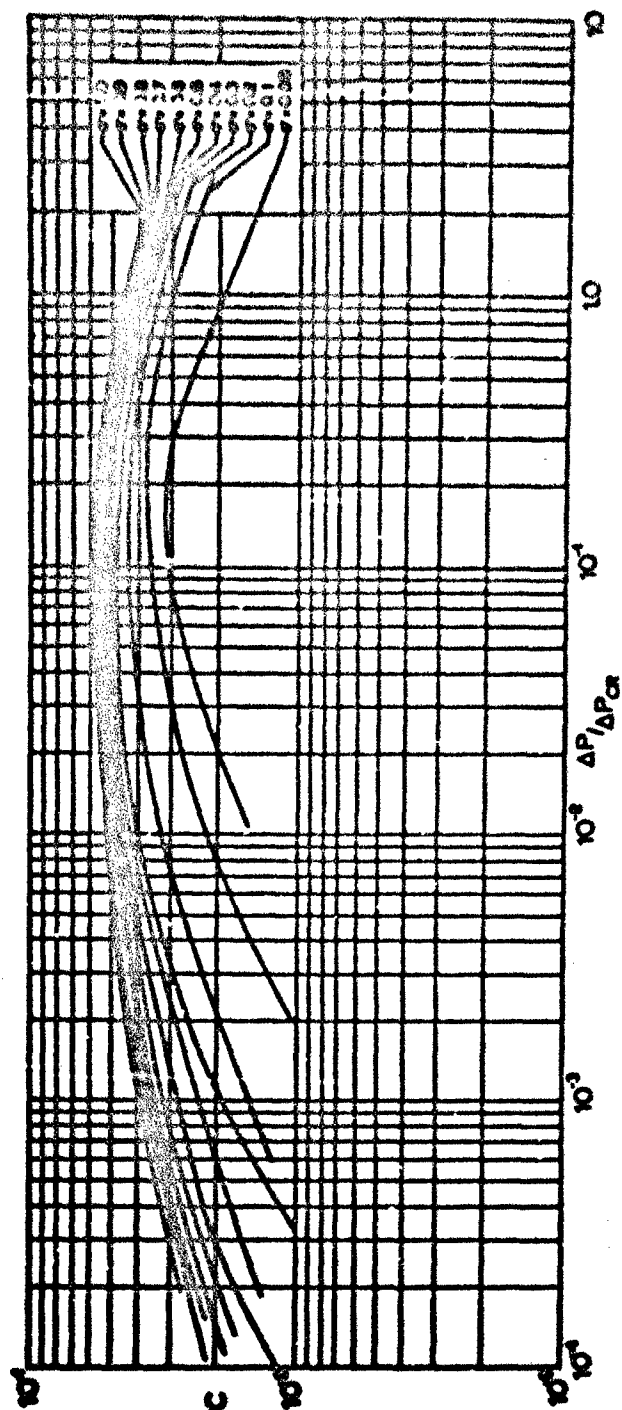
FIG 22 EFFECTIVE POROSITY FOR MIL-C-7350B TYPE I, 90 lb/h NYLON

39

TABLE 7

EFFECTIVE POROSITY OF 200 lb/in NYLON CLOTH MIL-C-8021A, TYPE I, AT VARIOUS PRESSURE AND DENSITY RATIOS. ALL POINTS ARE AVERAGE OF SEVERAL EXPERIMENTAL VALUES

| $\frac{\Delta p/p}{\sigma}$	0.05	0.1	0.2	0.3	0.4	0.5	0.6	0.7	0.8	0.9	1.0
2.0000	.0069	.0081	.0103	.0107	.0115	.0119	.0123				
1.0000	.0090	.0113	.0132	.0143	.0158	.0165	.0173	.0176	.0178	.0184	.0191
0.7000	.0100	.0116	.0139	.0151	.0167	.0175	.0184	.0186	.0188	.0199	.0204
0.3000	.0091	.0113	.0141	.0167	.0172	.0198	.0205	.0211	.0212	.0222	.0224
0.1000	.0065	.0095	.0121	.0155	.0171	.0187	.0197	.0205	.0210	.0222	.0231
0.0700	.0056	.00839	.0114	.0148	.0164	.0179	.0189	.0197	.0204	.0218	.0229
0.0300		.00582	.00941	.0126	.0142	.0156	.0169	.0176	.0183	.0199	.0212
0.0100			.0066	.0088	.0100	.0125	.0139	.0148	.0157	.0164	.0178
0.0070			.00565	.0076	.0096	.0111	.0128	.0135	.0148	.0153	.0165
0.0030				.00519	.0068	.0082	.00945	.0109	.0119	.0127	.0137
0.0010					.0042	.00518	.0060	.0070	.0081	.0089	.0098
0.0007							.0050	.0058	.0068	.00757	.0081
0.0004									.0051	.0056	.00605
0.0002											
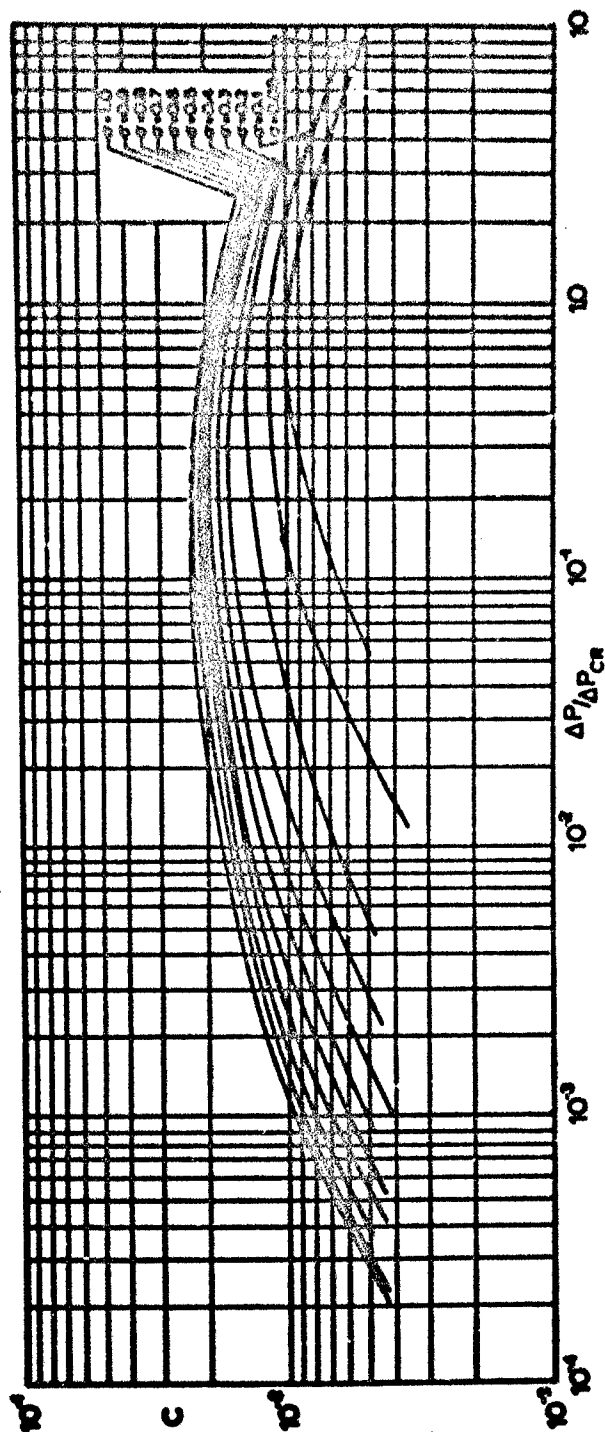
FIG 23   EFFECTIVE POROSITY VERSUS PRESSURE RATIO FOR ML-C-8021A, TYPE I , .200 E/In NYLON

41

TABLE 8

EFFECTIVE POROSITY OF 300 lb/in NYLON CLOTH, MIL-C-8021A, TYPE II, AT VARIOUS PRESSURE AND DENSITY RATIOS

ALL POINTS ARE AVERAGE OF SEVERAL EXPERIMENTAL VALUES

| $\Delta P/P$	0.05	0.1	0.2	0.3	0.4	0.5	0.6	0.7	0.8	0.9	1.0
2.0000	.0107	.0125	.0134	.0139	.0150	.0156	.0165	.0169			
1.0000	.0126	.0150	.0164	.0171	.0186	.0194	.0200	.0206	.0211	.0219	.0218
0.7000	.0137	.0158	.0181	.0189	.0203	.0212	.0219	.0224	.0229	.0228	.0224
0.3000	.0142	.0168	.0211	.0219	.0237	.0248	.0253	.0262	.0268	.0275	.0271
0.1000	.0127	.0158	.0202	.0219	.0235	.0248	.0255	.0263	.0269	.0226	.0220
0.0700	.0115	.0149	.0197	.0216	.0232	.0242	.0251	.0259	.0264	.0275	.0275
0.0300	.00844	.0119	.0169	.0193	.0211	.0224	.0234	.0238	.0245	.0253	.0257
0.0100		.00782	.0131	.0159	.0176	.0189	.0199	.0206	.0213	.0219	.0223
0.0070		.00675	.0118	.0149	.0164	.0179	.0188	.0195	.0201	.0207	.0214
0.0030			.0091	.0123	.0141	.0157	.0163	.0171	.0173	.0181	.0191
0.0010				.0088	.0108	.0119	.0131	.0141	.0148	.0141	.0169
0.0007					.0091	.0107	.0118	.0128	.0137		
0.0004						.00855	.0099	.0109	.0118		
0.0002						.00768	.00899	.0099	.0103		
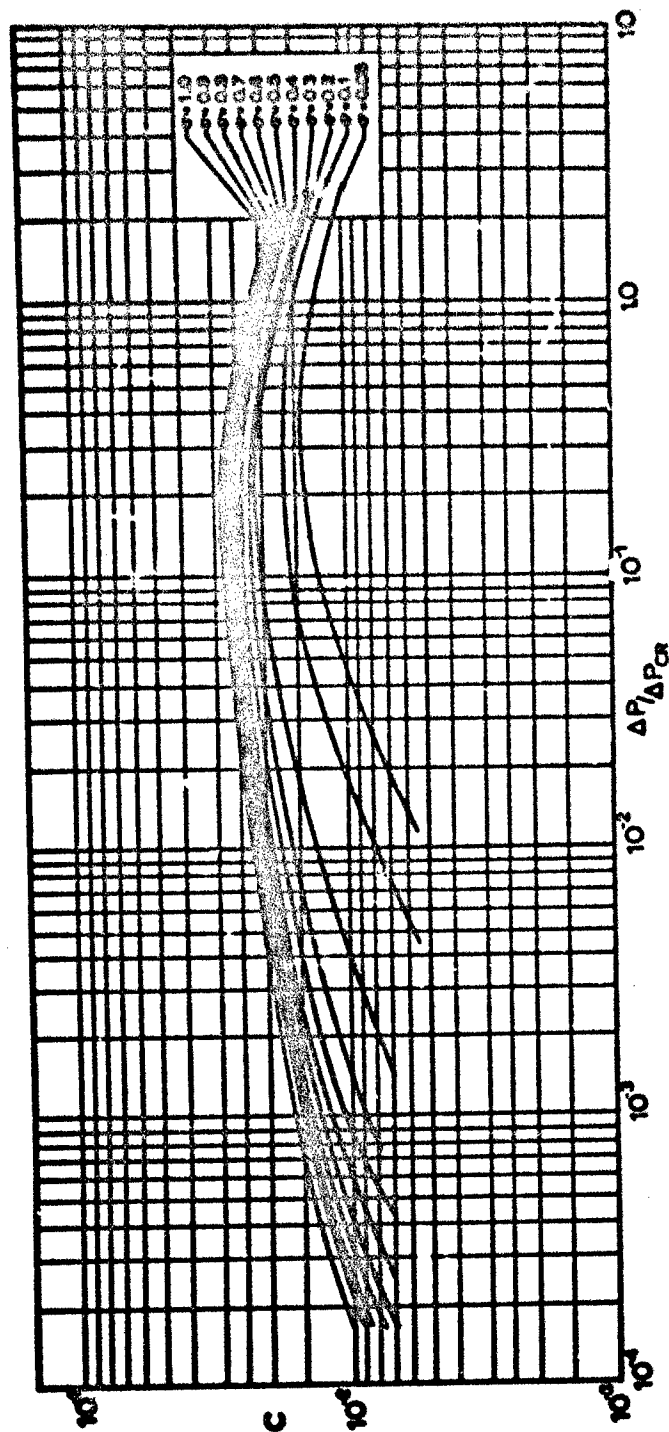
FIG 24   EFFECTIVE POROSITY VERSUS PRESSURE RATIO FOR ML-C-8021A, TYPE I, 300 Dn NYLON

TABLE 9

EFFECTIVE POROSITY OF 30x40 WIRE MESH AT VARIOUS PRESSURE AND DENSITY RATIOS

| ΔP/σ	0.05	0.1	0.3	0.5	1.0
2.0000		0.0247	0.0290	0	0.0200
1.0000	0.0253	0.0300	0.0375	0.0375	0.0375
0.7000	0.0251	0.0315	0.0405	0.0420	0.0420
0.3000	0.0216	0.0320	0.0440	0.0496	0.0496
0.1000	0.0150	0.0236	0.0410	0.0500	0.0519
0.0700	0.0127	0.0200	0.0383	0.0475	0.0513
0.0300	0.0088	0.0130	0.0308	0.0400	0.0500
0.0100		0.0068	0.0219	0.0305	0.0429
0.0070			0.0180	0.0278	0.0395
0.0030			0.0122	0.0214	0.0319
0.0010					0.0223
0.0007					0.0190

44
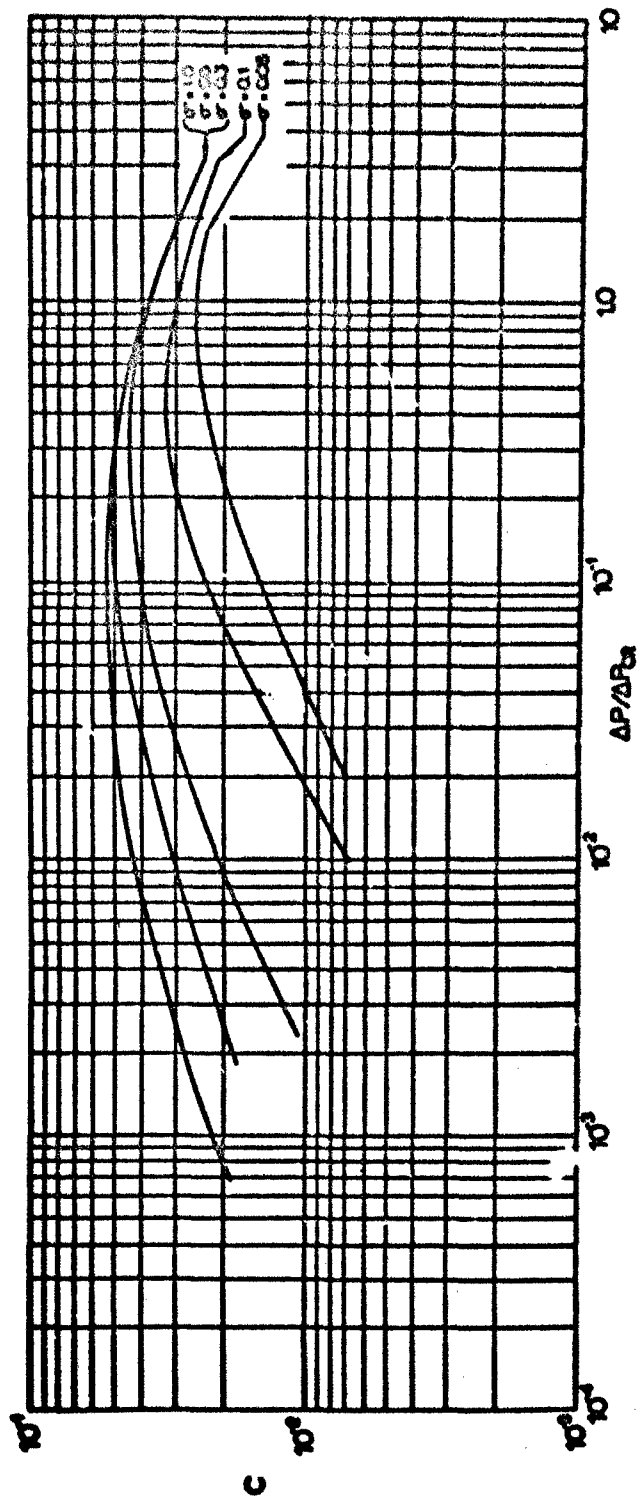
FIG 25 EFFECTIVE POROSITY VERSUS PRESSURE RATIO FOR 30X40 MESH STRANDED WEAVE WIRE SCREEN

45

TABLE 10

EFFECTIVE POROSITY OF 45% GEOMETRIC POROSITY PERLON CLOTH AT VARIOUS PRESSURE AND DENSITY RATIOS

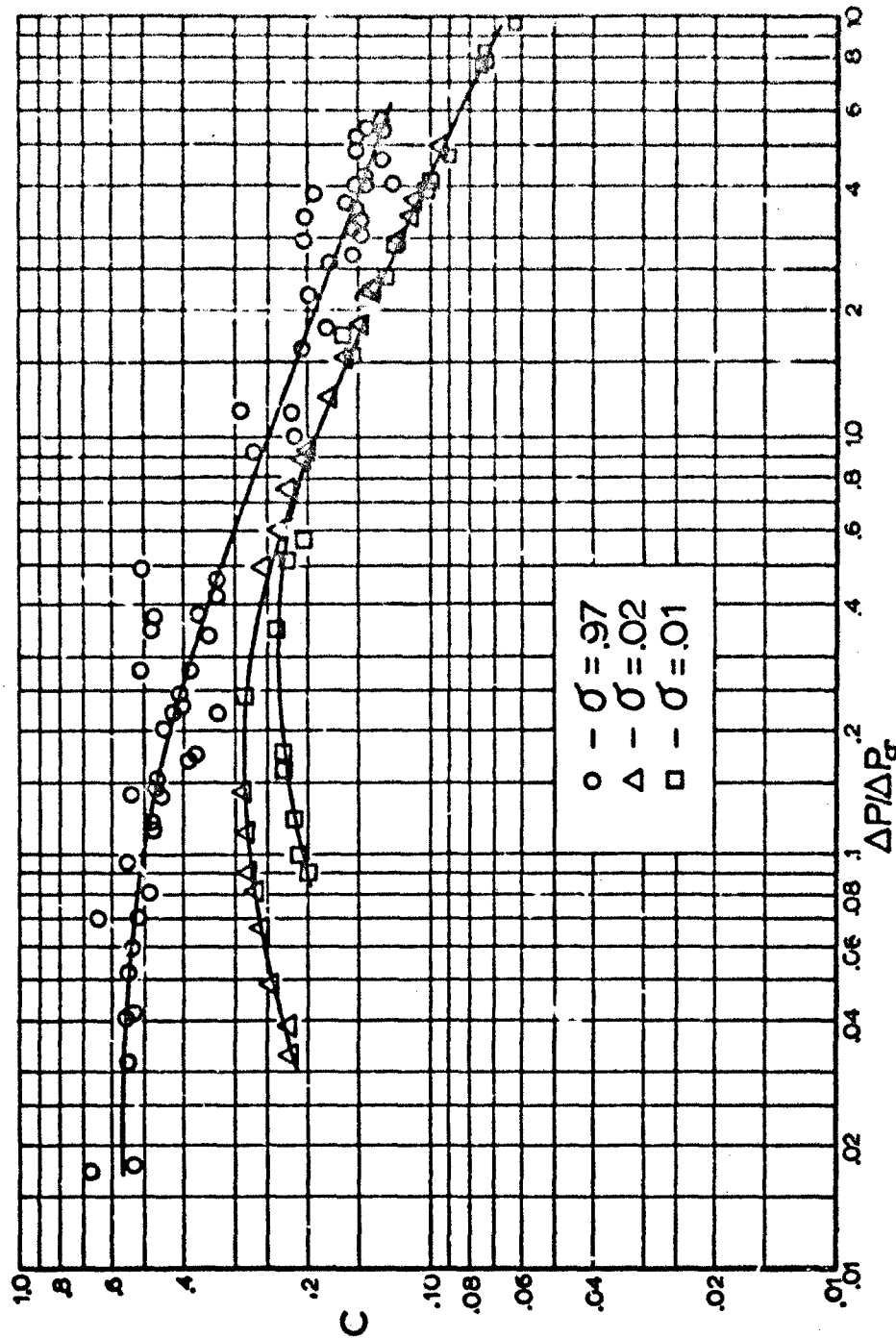| $\Delta P/\Delta P_{cr}$ \ σ	.01	.02	.97
7.0000	0.0780	0.0780	0.136
3.0000	0.116	0.116	0.164
2.0000	0.137	0.137	0.185
1.0000	0.190	0.190	0.248
0.7000	0.215	0.215	0.280
0.3000	0.238	0.275	0.386
0.1000	0.204	0.276	0.500
0.0700		0.260	0.515
0.0300			0.561

FIG 26. EFFECTIVE POROSITY VERSUS PRESSURE RATIO
FOR 45 % GEOMETRIC POROSITY PERLON

47

VII. REFERENCES

1. G. A. Hellenbeck. The Magnitude and Duration of Parachute Opening Shocks at Various Altitudes and Air Speeds, AF Memorandum Report ENG 49-696-66, 1947.

2. Henry F. Freeman and I. Rosenberg. High Altitude and High Air Speed Tests of Standard Parachute Canopies, AFFTC TR 58-32, ASTIA Document No AD 152 286.

3. T. Karman. Note on Analysis of the Opening Shock of Parachutes at Various Altitudes, Army Air Corps Scientific Advisory Group, 1945.

4. R. Ludwig and W. Heins. Theoretische Untersuchungen zur dynamischen Stabilitaet von Fallschirmen, Deutsche Forschungsanstalt fuer Luft- und Raumfahrt, Braunschweig, Germany, 1962.

5. H. G. Heinrich. Experimental Parameters in Parachute Opening Theory, Bulletin of the 19th Symposium on Shock and Vibration, 1953, Office of the Secretary of Defense, Washington, D. C.

6. M. J. Goglia, H. W. S. LaVier, and C. D. Brown. Air Permeability of Parachute Cloths, Technical Research Journal, April, 1965.

7. H. D. Melzig. Ueber ein neues Verfahren fuer die Pruefung der Luftdurchlaessigkeit und der elastischen Eigenschaften von Fallschirmgeweben, Deutsche Forschungsanstalt fuer Luftfahrt, E. V., Braunschweig, Germany, DFL, Bericht, Nr. 146, 1961.

8. F. O'Hara. Notes on the Opening Behavior and the Opening Forces of Parachutes, Journal of the Royal Aeronautical Society, London, England, 1949.

9. B. Eckert and F. Pfluger. The Resistance Coefficient of Commercial Round Wire Grids, NACA TM 1003, January, 1942.

10. S. F. Hoerner. Aerodynamic Drag (published by author), 1958.

11. G. . . Schubauer, W. G. Spengenburg, and P. S. Klebanoff. Aerodynamic Characteristics of Damping Screens, National Bureau of Standards, NACA TN 2001, January, 1950.

12. D. E. Johnson, E. H. Newton, E. R. Benton, L. E. Ashman, and D. A. Knapton. Metal Filaments for High Temperature Fabrics, ASD TR 62-180, 1962.

13. H. Schlichting. *Boundary Layer Theory*, McGraw Hill, New York, 1955.

14. John L. Hodgson. *Similarity Parameters of Nozzle and Orifice Flow*, Transactions of the ASME, 1929.

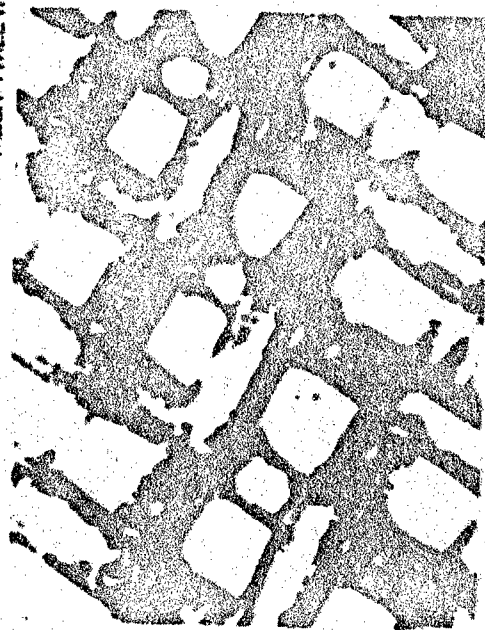15. R. C. Binder. *Fluid Mechanics*, Third Edition, Prentice-Hall, Inc., Englewood Cliffs, 1956.

1. Lichert, E. K.: Air Permeability of Woven Fabrics
   with Respect to Compressibility and Viscosity Effects,
   Master's Thesis, University of Minnesota, Department
   of Aeronautics and Engineering Mechanics, 1962.

2. Seshadi, Brown, Baker, Krizig, Mellen: Air Flow Char-
   acteristics of Parachute Fabrics at Simulated High
   Altitudes, WADC TR 59-374, 1960.

3. Smetana, F. O.: A Theoretical and Experimental Study
   of Gas Flow Through Cloth Over a Range of Pressures
   and Temperatures, ASD TR 61-192, 1961.

4. Baker, W. S. and Kaswell, E. R.: Handbook of Fibrous
   Materials, WADD TR 60-584, 1961.

5. Coplan. M. J. and Freeston, W. D.: High Speed Flow
   and Aerodynamic Heating Behavior of Porous Structures,
   WADD TN 61-58, 1961.

6. Heinrich, H. G.: The Effective Porosity of Parachute
   Cloth, Zeitschrift fuer Flugwissenschaften, WGLR,
   Germany, 1963.

7. Melzig, H. D.: Ein Beitrag zur Effektiven Porositaet
   von Fallschirmgeweben, Deutsche Forschungsanstalt fuer
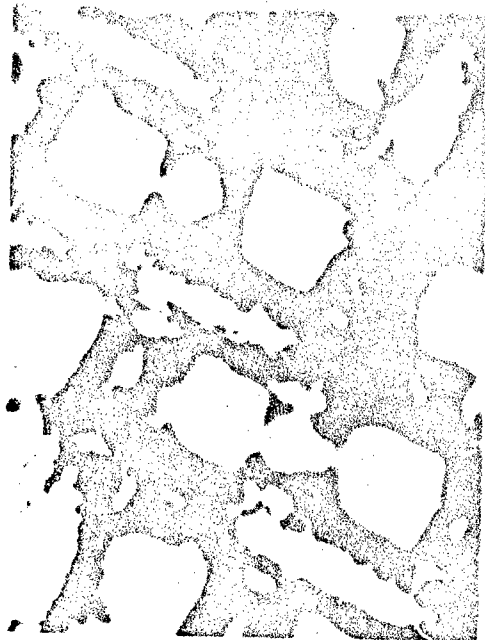   Luft- und Raumfahrt, Braunschweig, Germany, 1964.

APPENDIX

RESULTS OF AIR FLOW MEASUREMENTS OF
VARIOUS WIRE SCREENS

16% GEOMETRICAL POROSITY 60x60 MESH TWILL WEAVE
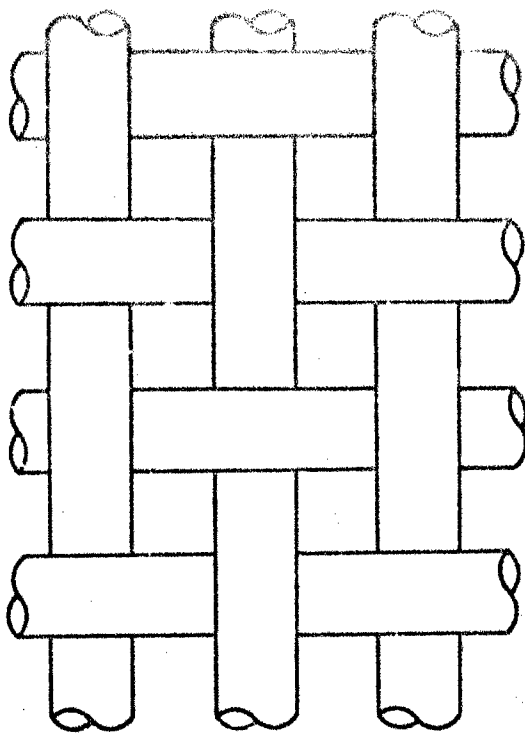
25% GEOMETRICAL POROSITY 50x50 MESH SQUARE WEAVE

11.7% GEOMETRICAL POROSITY 60x60 MESH TWILL WEAVE
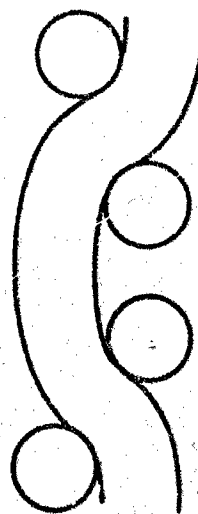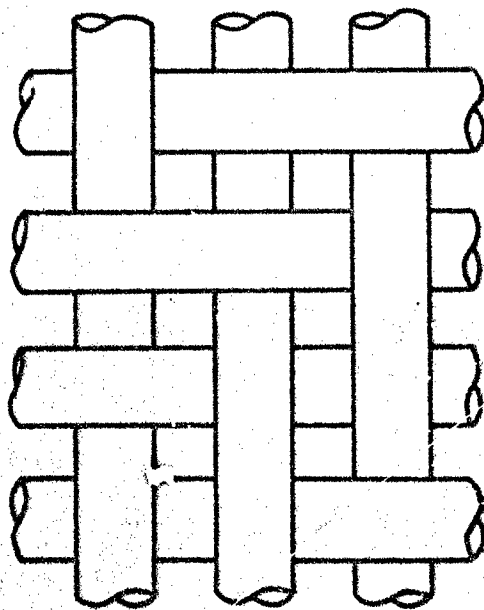
19.4% GEOMETRICAL POROSITY 80x80 MESH TWILL WEAVE

FIG 27 MICROSCOPIC PHOTOGRAPHS OF VARIOUS WIRE SCREENS

52

SQUARE WEAVE

TWILL WEAVE

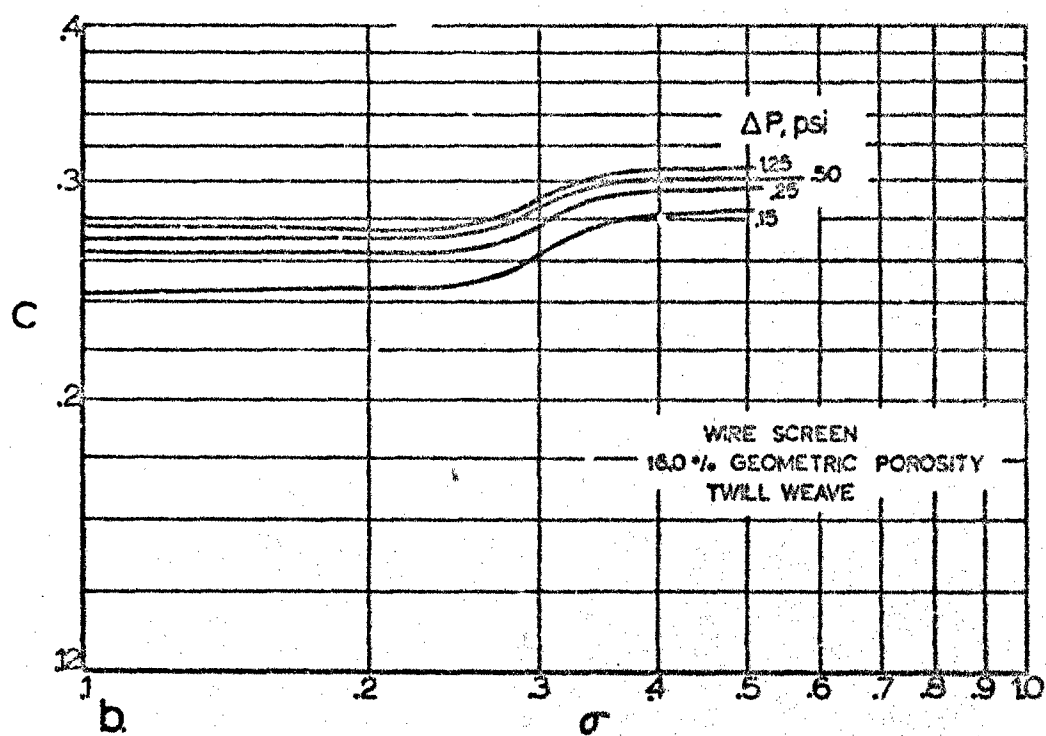FIG 28. SCHEMATIC WIRE SCREEN CHARACTERISTICS

53

FIG 29. a. and b.   EFFECTIVE POROSITY
VERSUS AIR DENSITY RATIO FOR
VARIOUS WIRE SCREENS

54

FIG 29 c. and d. EFFECTIVE POROSITY VERSUS AIR DENSITY RATIO FOR VARIOUS WIRE SCREENS
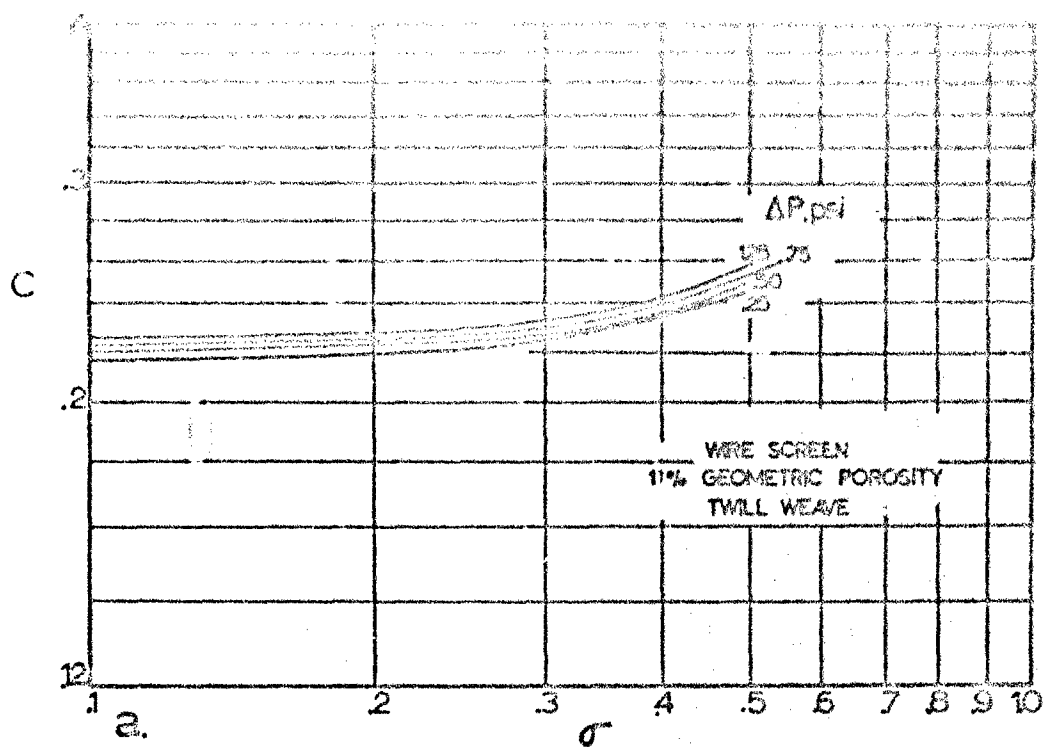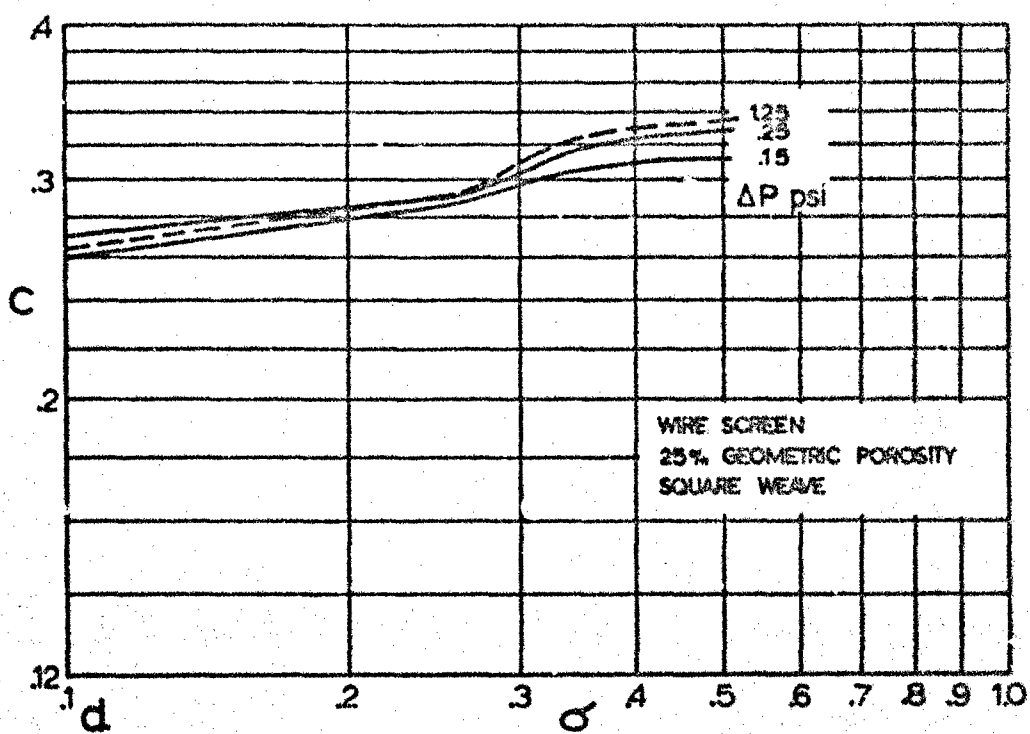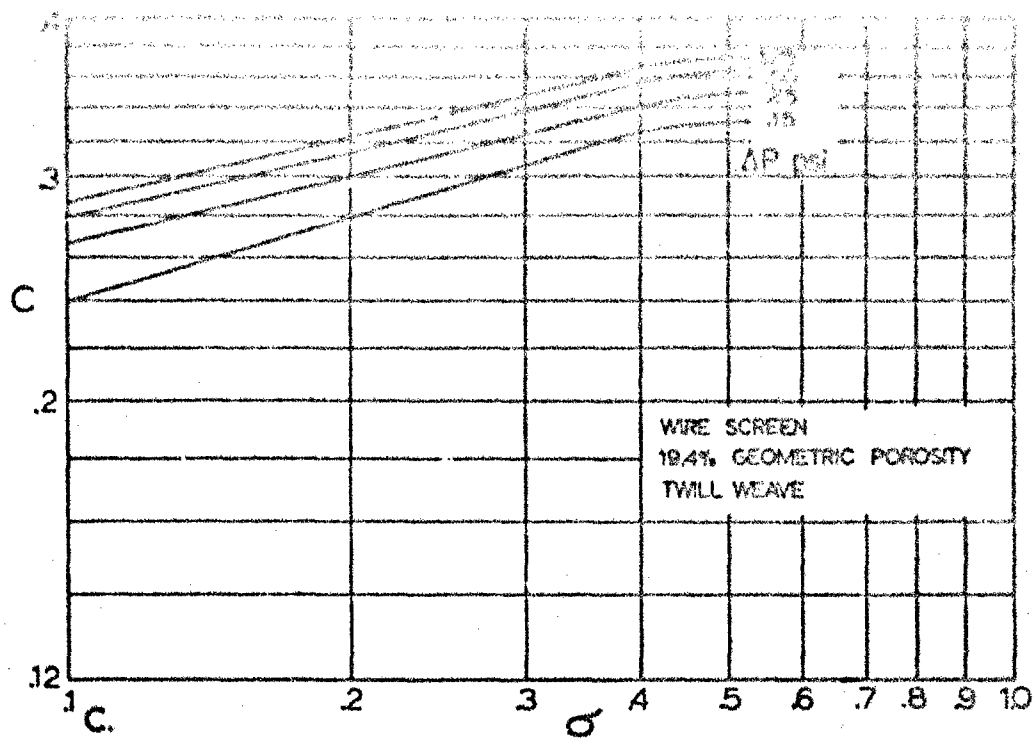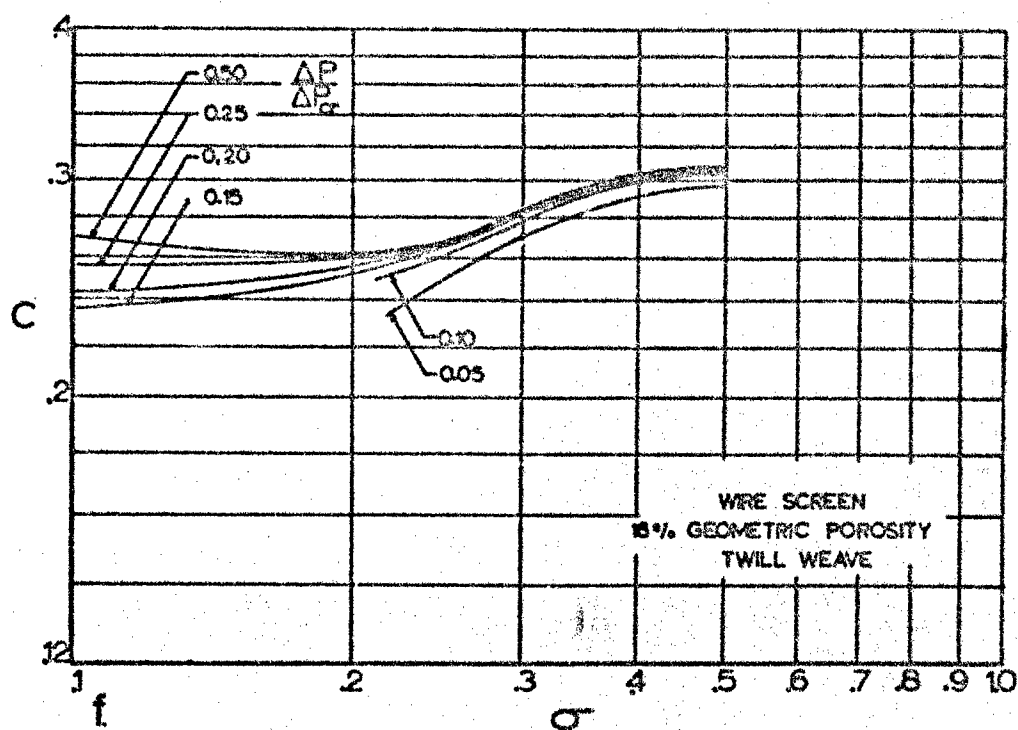
FIG 29 e and f.   EFFECTIVE POROSITY
VERSUS AIR DENSITY RATIO FOR
VARIOUS WIRE SCREENS

FIG 29. g. and h.   EFFECTIVE POROSITY
VERSUS AIR DENSITY RATIO FOR
VARIOUS WIRE SCREENS
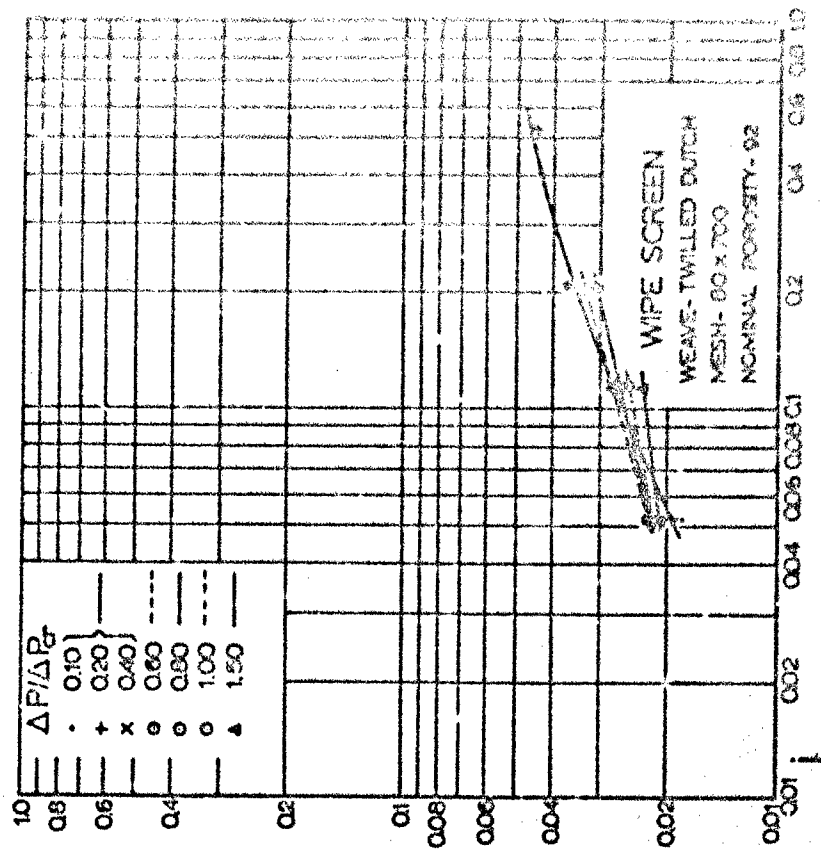
FIG. 29. i and j EFFECTIVE POROSITY VERSUS AIR DENSITY RATIO FOR VARIOUS WIRE SCREENS

Left chart (i):

WIRE SCREEN
WEAVE - PLAIN DUTCH
MESH - 50 x 50
NOMINAL POROSITY - 77.4

$\Delta P/\Delta P_{cr}$	
•	0.10
+	0.20
x	0.40
⊕	0.60

Right chart (j):

WIRE SCREEN
WEAVE - TWILLED DUTCH
MESH - 80 x 700
NOMINAL POROSITY - 92

$\Delta P/\Delta P_{cr}$	
•	0.10
+	0.20
x	0.40
⊕	0.60
◉	0.80
○	1.00
◄	1.50
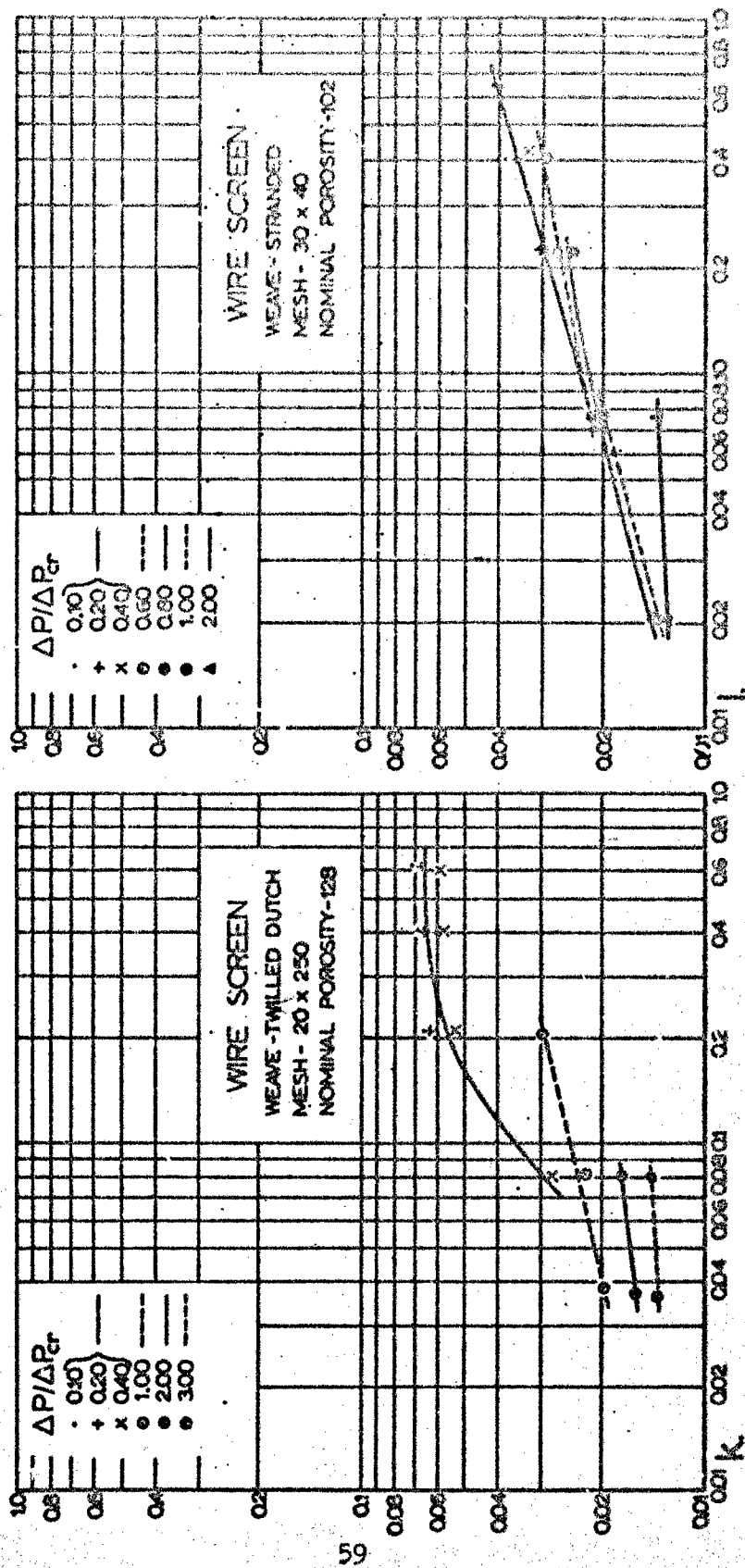
FIG 29 k and l EFFECTIVE POROSITY VERSUS AIR DENSITY RATIO FOR VARIOUS WIRE SCREENS

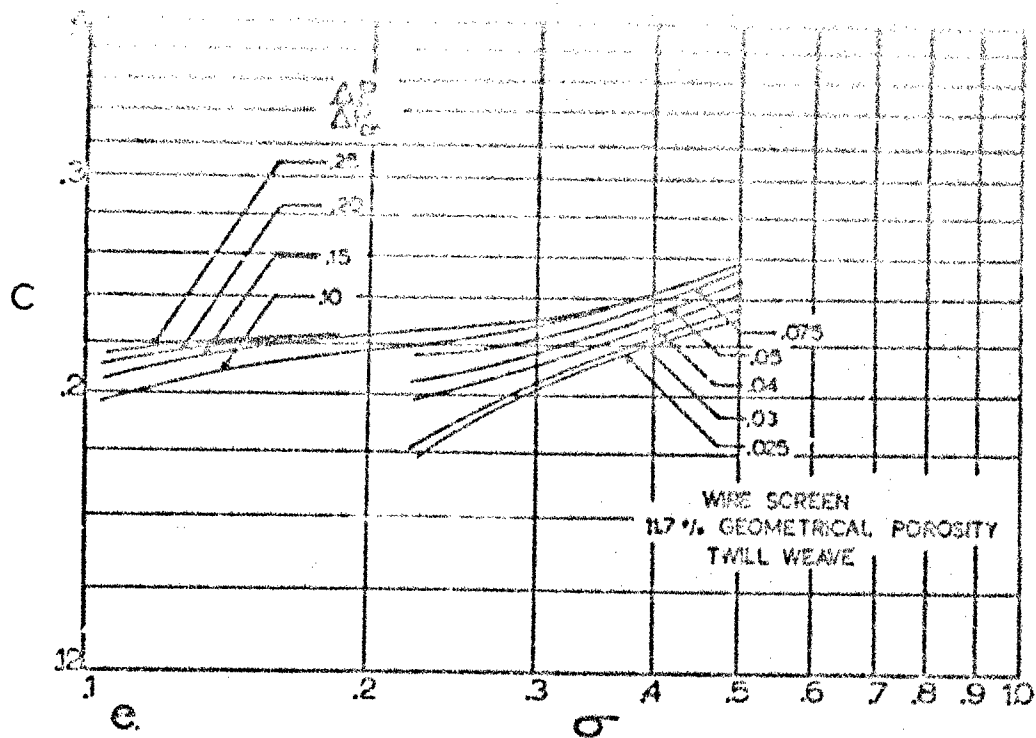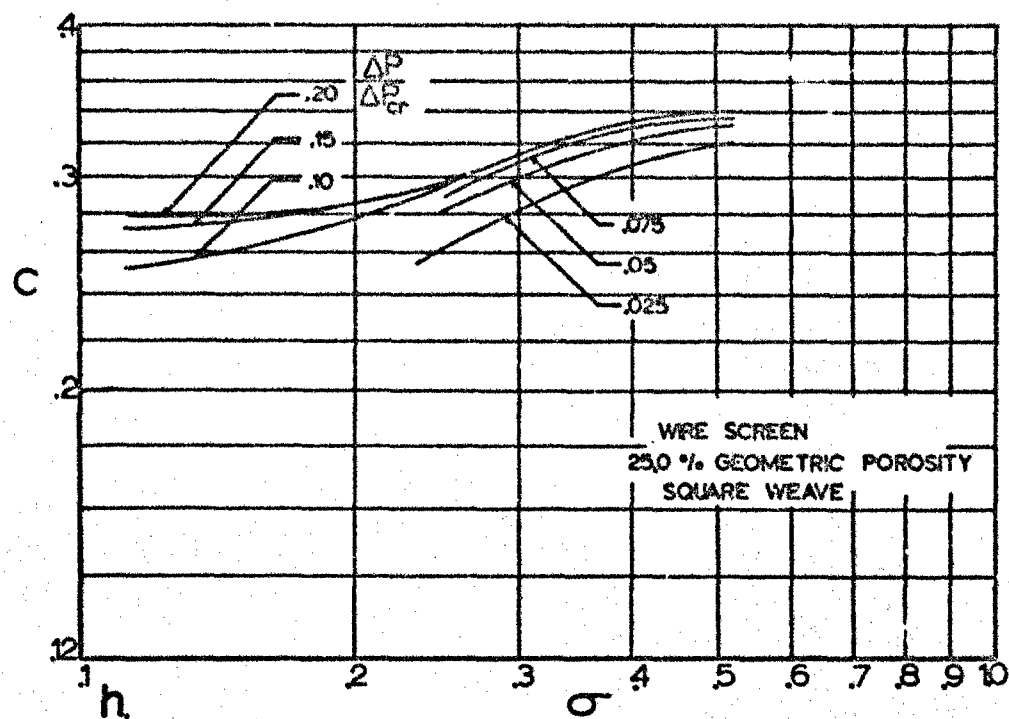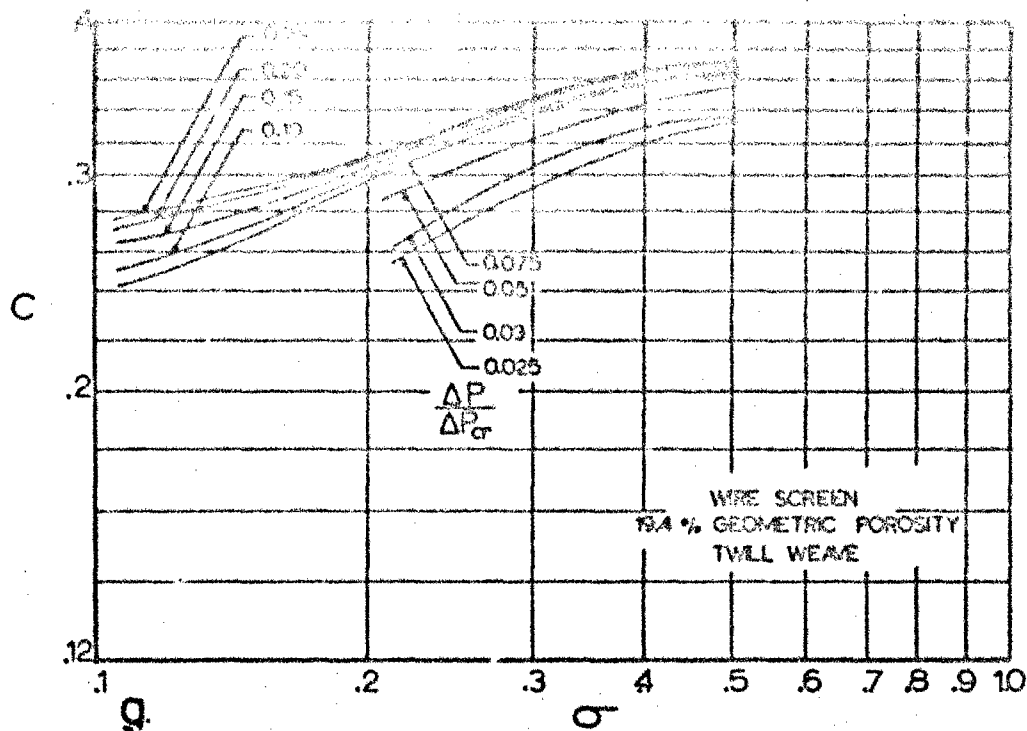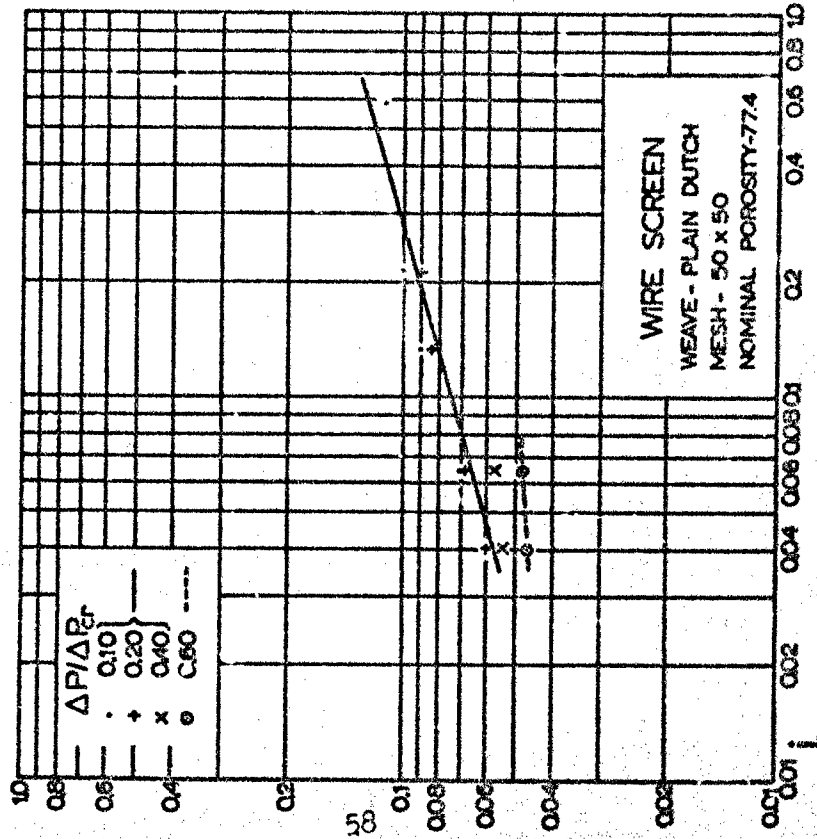## DOCUMENT CONTROL DATA - R&D

(Security classification of title, body of abstract and indexing annotation must be entered when the overall report is classified)

1. ORIGINATING ACTIVITY (Corporate author)	2a. REPORT SECURITY CLASSIFICATION
University of Minnesota Minneapolis 14, Minnesota	Unclassified
	2b. GROUP n/a

3. REPORT TITLE

The Effective Porosity of Parachute Cloth

4. DESCRIPTIVE NOTES (Type of report and inclusive dates)

Final report 15 April 63 - 15 April 65

5. AUTHOR(S) (Last name, first name, initial)

Heinrich, Helmut G

6. REPORT DATE	7a. TOTAL NO. OF PAGES	7b. NO. OF REFS
January 1966	59	15
8a. CONTRACT OR GRANT NO. AF33(657)-11184	9a. ORIGINATOR'S REPORT NUMBER(S)	
b. PROJECT NO. 6065	AFFDL-TR-65-102	
c. Task No 606503	9b. OTHER REPORT NO(S) (Any other numbers that may be assigned this report)	
d.		

10. AVAILABILITY/LIMITATION NOTICES
Qualified requesters may obtain copies of this report from DDC. This document is subject to special export controls and each transmittal to foreign governments or foreign nationals may be made only with prior approval of the AF Flight Dynamics Laboratory.

11. SUPPLEMENTARY NOTES	12. SPONSORING MILITARY ACTIVITY
None	AFFDL (FDFR) WPAFB, Ohio

13. ABSTRACT

Stability, drag, and opening characteristics of solid cloth parachutes change with altitude. Similar changes can be observed at a given altitude by when the air permeability or porosity of the cloth is being varied. In this study it is shown that the porosity of a given cloth changes effectively with the density and the compressibility of the air. The effective porosity is related to Reynolds and Mach numbers and it was found that the flow of the air through the cloth is in general turbulent but may approach under certain circumstances a laminar flow character.

Tables and graphs showing the effective porosity of four common types of parachute cloth and of one type of a perlon screen with 45% geometric porosity, as well as equations and coefficients which permit under certain simplifying assumptions the calculation of the effective porosity are presented.

DD FORM 1473 JAN 64

14	LINK A		LINK B		LINK C	
KEY WORDS	ROLE	WT	ROLE	WT	ROLE	WT
Porosity						
Permeability						
Effect of density						
Effect of compressibility						
Parachute cloth						
Perlon screen						

INSTRUCTIONS

1. ORIGINATING ACTIVITY: Enter the name and address of the contractor, subcontractor, grantee, Department of Defense activity or other organization (corporate author) issuing the report.

2a. REPORT SECURITY CLASSIFICATION: Enter the overall security classification of the report. Indicate whether "Restricted Data" is included. Marking is to be in accordance with appropriate security regulations.

2b. GROUP: Automatic downgrading is specified in DoD Directive 5200.10 and Armed Forces Industrial Manual. Enter the group number. Also, when applicable, show that optional markings have been used for Group 3 and Group 4 as authorized.

3. REPORT TITLE: Enter the complete report title in all capital letters. Titles in all cases should be unclassified. If a meaningful title cannot be selected without classification, show title classification in all capitals in parenthesis immediately following the title.

4. DESCRIPTIVE NOTES: If appropriate, enter the type of report, e.g., interim, progress, summary, annual, or final. Give the inclusive dates when a specific reporting period is covered.

5. AUTHOR(S): Enter the name(s) of author(s) as shown on or in the report. Enter last name, first name, middle initial. If military, show rank and branch of service. The name of the principal author is an absolute minimum requirement.

6. REPORT DATE: Enter the date of the report as day, month, year; or month, year. If more than one date appears on the report, use date of publication.

7a. TOTAL NUMBER OF PAGES: The total page count should follow normal pagination procedures, i.e., enter the number of pages containing information.

7b. NUMBER OF REFERENCES: Enter the total number of references cited in the report.

8a. CONTRACT OR GRANT NUMBER: If appropriate, enter the applicable number of the contract or grant under which the report was written.

8b, 8c, & 8d. PROJECT NUMBER: Enter the appropriate military department identification, such as project number, subproject number, system numbers, task number, etc.

9a. ORIGINATOR'S REPORT NUMBER(S): Enter the official report number by which the document will be identified and controlled by the originating activity. This number must be unique to this report.

9b. OTHER REPORT NUMBER(S): If the report has been assigned any other report numbers (either by the originator or by the sponsor), also enter this number(s).

10. AVAILABILITY/LIMITATION NOTICES: Enter any limitations on further dissemination of the report, other than those

imposed by security classification, using standard statements such as:

(1) "Qualified requesters may obtain copies of this report from DDC."

(2) "Foreign announcement and dissemination of this report by DDC is not authorized."

(3) "U. S. Government agencies may obtain copies of this report directly from DDC. Other qualified DDC users shall request through
_____."

(4) "U. S. military agencies may obtain copies of this report directly from DDC. Other qualified users shall request through
_____."

(5) "All distribution of this report is controlled. Qualified DDC users shall request through
_____."

If the report has been furnished to the Office of Technical Services, Department of Commerce, for sale to the public, indicate this fact and enter the price, if known.

11. SUPPLEMENTARY NOTES: Use for additional explanatory notes.

12. SPONSORING MILITARY ACTIVITY: Enter the name of the departmental project office or laboratory sponsoring (paying for) the research and development. Include address.

13. ABSTRACT: Enter an abstract giving a brief and factual summary of the document indicative of the report, even though it may also appear elsewhere in the body of the technical report. If additional space is required, a continuation sheet shall be attached.

It is highly desirable that the abstract of classified reports be unclassified. Each paragraph of the abstract shall end with an indication of the military security classification of the information in the paragraph, represented as (TS), (S), (C), or (U).

There is no limitation on the length of the abstract. However, the suggested length is from 150 to 225 words.

14. KEY WORDS: Key words are technically meaningful terms or short phrases that characterize a report and may be used as index entries for cataloging the report. Key words must be selected so that no security classification is required. Identifiers, such as equipment model designation, trade name, military project code name, geographic location, may be used as key words but will be followed by an indication of technical context. The assignment of links, rules, and weights is optional.

GPO 886-551